Zootaxa 5620 (2): 230–254
https://www.mapress.com/zt/

Article

ISSN 1175-5326 (print edition)
ZOOTAXA
ISSN 1175-5334 (online edition)

https://doi.org/10.11646/zootaxa.5620.2.2
http://zoobank.org/urn:lsid:zoobank.org:pub:EEEE2656-E891-4DD3-A30A-4CF07019F1D7

An updated survey of molecular diversity in Madagascar's velvet geckos, genus *Blaesodactylus*, with description of a new species from the island's arid West

MIGUEL VENCES[1*], AURELIEN MIRALLES[1,2], IVAN INEICH[2], ANDOLALAO RAKOTOARISON[3,4], CHRISTIAN GLASENAPP[1], MARK D. SCHERZ[5], JÖRN KÖHLER[6], FRANK GLAW[7] & ACHILLE P. RASELIMANANA[8,9]

[1]*Zoologisches Institut, Technische Universität Braunschweig, Mendelssohnstr. 4, 38106 Braunschweig, Germany.*
m.vences@tu-braunschweig.de; https://orcid.org/0000-0003-0747-0817
christian.glasenapp@gmail.com; https://orcid.org/0009-0003-6145-8138
[2]*Institut de Systématique, Évolution, Biodiversité (ISYEB), Muséum national d'Histoire Naturelle, CNRS, Sorbonne Université, EPHE, Université des Antilles, 57 rue Cuvier, 75231 Paris cedex, France.*
ivan.ineich@mnhn.fr; https://orcid.org/0000-0003-1235-1505
miralles.skink@gmail.com; https://orcid.org/0000-0002-2538-7710
[3]*Mention Environnement, Université de l'Itasy, Faliarivo Ambohidanerana, 118 Soavinandriana Itasy, Madagascar.*
[4]*School for International Training, VN 41A Bis Ankazolava Ambohitsoa, Antananarivo, 101 Madagascar.*
andomailaka@gmail.com; https://orcid.org/0000-0003-2620-440X
[5]*Natural History Museum Denmark, University of Copenhagen, Universitetsparken 15, 2100, Copenhagen Ø, Denmark.*
mark.scherz@gmail.com; https://orcid.org/0000-0002-4613-7761
[6]*Hessisches Landesmuseum Darmstadt, Friedensplatz 1, 64283 Darmstadt, Germany.*
joern.koehler@hlmd.de; https://orcid.org/0000-0002-5250-2542
[7]*Zoologische Staatssammlung München (ZSM-SNSB), Münchhausenstr. 21, 81247 München, Germany.*
glaw@snsb.de; https://orcid.org/0000-0003-4072-8111
[8]*Mention Zoologie et Biodiversité Animale, Université d'Antananarivo, BP 906, Antananarivo, 101 Madagascar.*
[9]*Association Vahatra, Lot V A 38 LBA Ter Ambohidempona Tsiadana, BP 3972, Antananarivo, 101 Madagascar.*
raselimananaachille@gmail.com; https://orcid.org/0000-0003-1610-7307
**Corresponding author.*

Abstract

Madagascar velvet geckos, genus *Blaesodactylus*, are classified in six species distributed over low-elevation sites across most of Madagascar. Based on DNA sequences of one mitochondrial and two nuclear-encoded gene fragments obtained from numerous newly collected tissue samples, we provide an updated review of their molecular variation. Our genetic screening confirms an extended distribution of *B. ambonihazo*, so far only known from its type locality Ankarafantsika, now reaching northwards to the Sahamalaza Peninsula. Compared to previously available molecular data, we also verify minor range extensions of *B. boivini* (southeastwards to Bezavona), *B. antongilensis* (northwards to the Marojejy Massif), and the *B. sakalava* complex. Samples assigned to *B. sakalava* according to current taxonomy fell into two mitochondrial sister lineages differing by about 8.5% pairwise distances in the 16S rRNA gene, lack of haplotype sharing in the nuclear-encoded CMOS gene, and various subtle but consistent differences in body proportions and scalation. We conclude that the lineage occurring in the South of Madagascar, encompassing known locations south of Morombe, corresponds to *B. sakalava* sensu stricto based on its type locality and morphological characters of its name-bearing type; and describe the lineage occurring in the West of Madagascar north of Morombe as a new species, *B. ganzhorni* **sp. nov**.

Key words: Squamata, Gekkonidae, *Blaesodactylus sakalava*, *Blaesodactylus ganzhorni* **sp. nov.**, *Blaesodactylus ambonihazo*, *Blaesodactylus boivini*, distribution, taxonomy

Introduction

Madagascar is home to a diversified fauna of gekkonid lizards. Of the currently ca. 440 species of squamates occurring on Madagascar (Uetz 2024), 141 and thus about one third are geckos, of which the vast majority is endemic to the island (Bauer *et al.* 2022). According to the most recent revisions (Bauer *et al.* 2011; Jono *et al.*

 Accepted by A. Bauer: 2 Mar. 2025; published: 9 Apr. 2025

2015; Ineich *et al.* 2016), the genus *Blaesodactylus* contains six nominal species of Madagascar velvet geckos, all of which are Madagascar-endemic: *B. ambonihazo* Bauer, Glaw, Gehring and Vences, 2011; *B. antongilensis* (Böhme and Meier, 1980); *B. boivini* (Duméril, 1856); *B. microtuberculatus* Jono, Bauer, Brennan and Mori, 2015; *B. sakalava* (Grandidier, 1867); and *B. victori* Ineich, Glaw and Vences, 2016. All of these are large-sized, mostly nocturnal geckos (Fig. 1). The various species of *Blaesodactylus*, which have long been considered as congeneric with African geckos of the genus *Homopholis* (Greenbaum *et al.* 2007), inhabit either rainforest, dry deciduous forest, or spiny thicket biomes of Madagascar, and only little information is available on their natural history (e.g., Ikeuchi & Mori 2014).

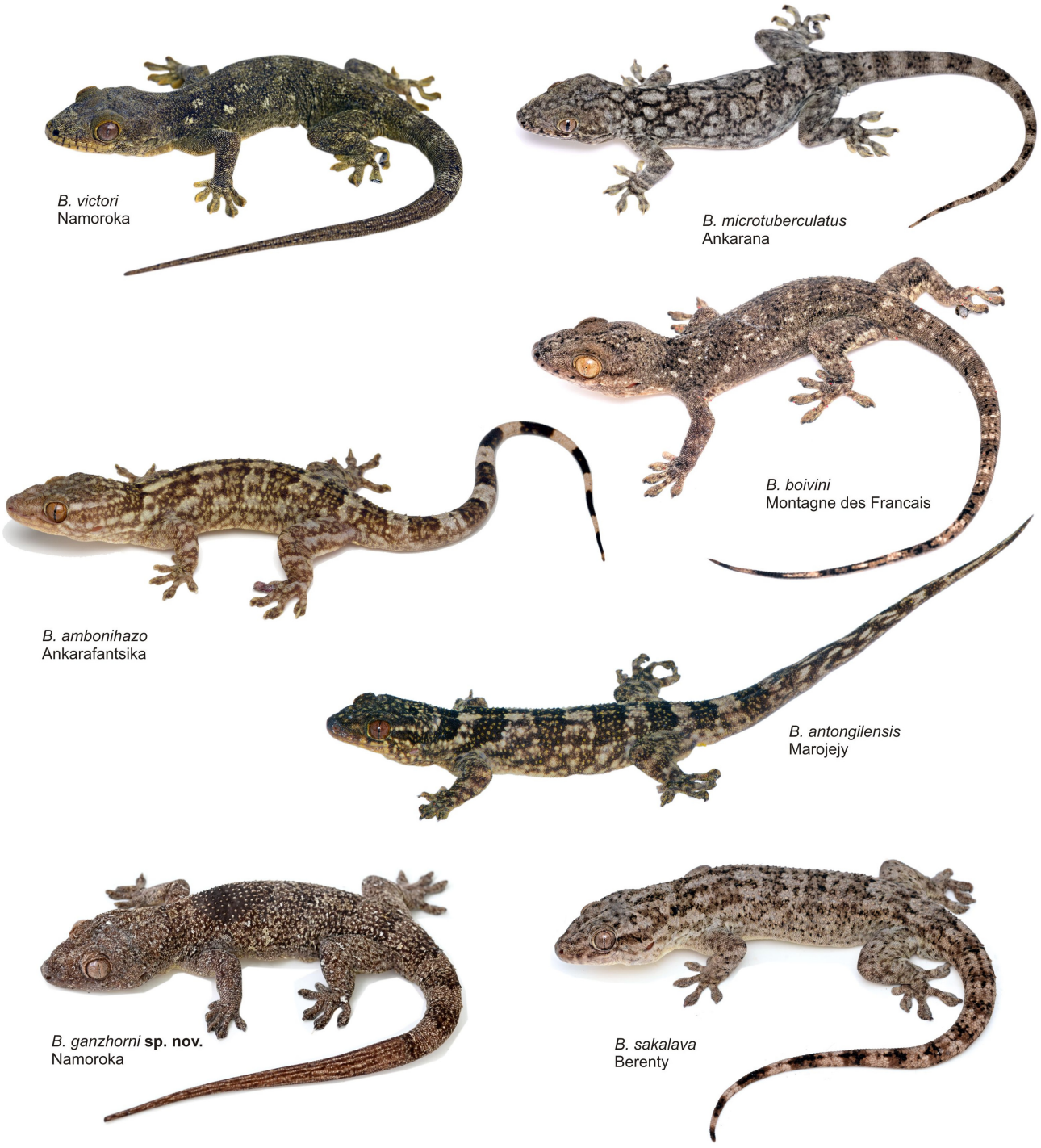

FIGURE 1. Representative specimens of all known species of Madagascar velvet geckos, genus *Blaesodactylus*, in life. Depicted *B. ganzhorni* **sp. nov.** shows paratype ZSM 62/2023 (ZCMV 15810).

Although most species of *Blaesodactylus* can rather easily be identified and distinguished by their general appearance, morphological differences among species are in some cases rather subtle, restricted to differences in body size, head scalation or prominence of tubercular dorsal scales. Molecular data from DNA sequences of mitochondrial and nuclear-encoded gene fragments have, however, confirmed substantial genetic divergence among all currently recognized species, thus supporting the current classification.

Given the superficial morphological similarity of most species of *Blaesodactylus*, it is not surprising that the detailed distribution range, and range-wide genetic and morphological variation, is insufficiently known for several species. For instance, two species (*B. microtuberculatus* and *B. victori*) are so far known from single locations only, and previous studies have shown a substantial genetic variation among samples assigned to *B. sakalava*, a species widespread in western and southern Madagascar (Bauer *et al.* 2011; Jono *et al.* 2015; Ineich *et al.* 2016).

In the present study, we aim to fill gaps in the knowledge on the systematics of *Blaesodactylus*. We built upon a large set of samples collected by various research teams across Madagascar, in particular, a dense sampling in the West, Northwest and South of the island. We extended the available molecular data set for the new samples and for one additional nuclear-encoded marker and examined morphology of representative individuals assigned to *B. sakalava.* From these analyses we refine and extend the distribution ranges of *B. ambonihazo*, *B. antongilensis* and *B. sakalava*, and provide evidence that the populations assigned to *B. sakalava* represent a species complex (here named the *B. sakalava* complex); we conclude that populations from the northern part of the range of this complex represent a new species which is formally named and described herein.

Materials and Methods

This study is based on specimens and samples of *Blaesodactylus* collected during multiple expeditions of various research teams. In most cases, geckos were captured during opportunistic nocturnal searches with the aid of flashlights. Representative individuals were photographed alive immediately after capture using different digital cameras. Voucher specimens were anesthetized and subsequently euthanized by overdoses of approved anesthetics, either by injections of sodium pentobarbital, or MS222, ketamine, or by application of lidocaine in the buccal cavity. Tissue samples were taken from the euthanized specimens and preserved in separate tubes filled either with absolute ethanol or EDTA. Subsequently, specimens were fixed in either 10% formalin or 95% ethanol and later preserved in 75% ethanol. Voucher specimens examined in this study for morphological and/or molecular characters are deposited in the collections of the Zoologische Staatssammlung München (ZSM), the Muséum National d'Histoire Naturelle, Paris (MNHN), and the Mention Zoologie et Biodiversité Animale of the University of Antananarivo (UADBA). The acronyms APR, FGMV, FGZC, JNM, MSZC, PSG, MVTIS and ZCMV correspond to field series or laboratory numbers of Achille P. Raselimanana, Frank Glaw, Joachim Nopper, Mark D. Scherz, Philip-Sebastian Gehring, and Miguel Vences, respectively; field numbers of Ivan Ineich are preceded by "I"; and samples provided by the team of the NGO Madagasikara Voakajy are marked MaVoa. Furthermore, some sequences downloaded from GenBank have voucher or sample numbers labelled KUZ (Zoological Collection of Kyoto University, Japan) and WRBM (William Roy Branch Madagascar Field Series). Specimens in the UADBA collection are in many cases not provided with final catalogue numbers due to lack of curatorial resources but are identifiable by their distinct field number tags; we therefore report these specimens as UADBA-APR (for specimens with APR field numbers) and UADBA-ZCMV (for specimens with ZCMV field numbers). Biogeographic regions of Madagascar are named following the scheme of Boumans *et al*. (2007).

We took a series of morphometric measurements and meristic counts from representative specimens of the *B. sakalava* complex. Measurements (all in mm) taken with a vernier caliper to the nearest 0.1 mm were as follows: SVL, snout–vent length, tip of snout to center of cloacal orifice; TAL, tail length from center of cloaca to tip of tail; HIL, hindlimb length from body insertion to longest toe including claw; HW, head width at broadest point, i.e., just behind the eye; ED, antero-posterior (horizontal) eye diameter; SED, distance from snout tip to center of ear opening. Scale counts were INFL, number of infralabial scales; SUPL, number of supralabial scales; LongTub, number of dorsal tubercles in a longitudinal row from head to start of tail (i.e., to a position roughly corresponding to cloacal orifice); LCDS, number of dorsal scales along the body, medially from first scale after the internasals to the first scale row or whorl of the tail; LCVS, longitudinal count of the number of ventral scales from the mental scale to the cloaca. LongTub, LCDS and LCVS were counted from high-resolution digital images taken from the preserved specimens. The width of the mental scale at its posterior edge, and the length of the first postmental scale was measured from (unscaled) photos using ImageJ (Schneider *et al*. 2012), and

a ratio between both measures calculated. Statistical analysis was carrried out in Statistica v7.1 (Statsoft Inc). Numerous additional meristic characters were explored to find possible diagnostic differences between the two molecular lineages that we identified in the *B. sakalava* complex. They are reported without abbreviation in the holotype description and diagnosis below.

Molecular genetic study follows previous approaches (Bauer *et al.* 2011; Ineich *et al.* 2016) in targeting a fragment of the mitochondrial NADH Dehydrogenase gene, subunit 4 (ND4) and a segment of the nuclear-encoded Recombination-activating Gene I (RAG1). These were supplemented with new sequences of fragments of the nuclear-encoded Oocyte Maturation Factor gene (CMOS) and (for 1–2 individuals per species) the mitochondrial genes for 12S rRNA (12S) and 16S rRNA (16S). DNA was extracted from tissue samples following a standard salt-extraction protocol (Bruford *et al.* 1992). The ND4 fragment (terminally including a segment of tRNAHis) was PCR-amplified with primers ND4 (CAC CTA TGA CTA CCA AAA GCT CAT GTA GA) and leutRNA (AGC CAT TAC TTT TAC TTG GAT TTG CAC C) (originally from Arevalo *et al.* 1994; modified primer sequences courtesy of Ed Louis, Omaha's Henry Doorly Zoo), and the following protocol: initial denaturation at 94°C for 90 sec, 33 cycles of denaturation at 94°C for 45 sec, annealing at 47°C for 45 sec, elongation at 72°C for 90 sec, followed by 10 minutes of final elongation 72°C, according to Bauer *et al.* (2011). The RAG-1 fragment was amplified using primers UropRAG1-F1 (GAA AAC CTG GAG CGG TAT GA) and UropRAG1-R1 (GCA ACT CTG CAA AAC GTT GA) and the following protocol: initial denaturation at 94°C for 120 sec, 39 cycles of denaturation at 94°C for 20 sec, annealing at 51°C for 50 sec, elongation at 72°C for 180 sec, followed by 10 minutes of final elongation at 72°C, according to Bauer *et al.* (2011). The CMOS fragment was amplified using primers CO8 (GCT TGG TGT TCA ATA GAC TGG) and CO9 (TTT GGG AGC ATC CAA AGT CTC) from Han *et al.* (2004), and the following protocol: initial denaturation at 94°C for 180 sec, 36 cycles of denaturation at 94°C for 45 sec, annealing at 51°C for 45 sec, elongation at 72°C for 60 sec, followed by 6 minutes of final elongation at 72°C. The 12S fragment was amplified using primers 16SAL (AAA CTG GGA TTA GAT ACC CCA CTA T) and 12SBH (GAG GGT GAC GGG CGG TGT GT), from Kocher *et al.* (1989), with the following cycling protocol: initial denaturation at 94°C for 90 sec, 33 cycles of denaturation at 94°C for 45 sec, annealing at 52°C for 45 sec, elongation at 72°C for 90 sec, and 300 sec of final elongation at 72°C. The 16S fragment using was amplified using primers 16SAL (CGC CTG TTT ATC AAA AAC AT) and 16SBH-new (CCT GGA TTA CTC CGG TCT GA), modified from Palumbi *et al.* (1991), with the following cycling protocol: initial denaturation at 94°C for 90 sec, 33 cycles of denaturation at 94°C for 45 sec, annealing at 55°C for 45 sec, elongation at 72°C for 90 sec, and 300 sec of final elongation at 72°C. Reaction mixes contained 1 µl template DNA, 0.25 µl of 10 µM dNTPs, 0.3 µl of each 10 µM Primer, 2.5 µl Colorless 5x GoTaq Reaction Buffer, and 0.1 µl GoTaq G2 DNA Polymerase (5 U/µl) in a total volume of 12.5 µl. Nucleotide debris was removed by adding 2.4 µl ExoSAP to 8 µl PCR (Bell 2008). Sequencing of purified PCR products was conducted on capillary sequencers by LGC Biosearch Technologies in Berlin, Germany. CodonCode Aligner 6.0.2 (CodonCode Corporation) was utilized to verify sequence quality of chromatograms and stretches of poor read quality were removed. New sequences were submitted to GenBank (accession numbers: PV130183–PV130367, PV156454–PV156466, and PV156467–PV156478), and complemented with sequences from previous studies (Bauer *et al.* 2011; Jono *et al.* 2015; Ineich *et al.* 2016) available from GenBank. A table with all sequences used and their accession numbers, as well as the tree files and alignments, are available from the Zenodo repository (https://doi.org/10.5281/zenodo.14889416).

We aligned DNA sequences using the G-INS-i option in MAFFT (Katoh & Standley 2013) as implemented in the program Concatenator (Vences *et al.* 2022a) and used the same program to concatenate the three mitochondrial gene fragments (ND4, 12S and 16S) for analysis. From the concatenated ND4 + 12S + 16S alignment we then reconstructed a Maximum Likelihood tree in RAxML (Stamatakis 2014) using raxmlGUI v. 2.0 (Edler *et al.* 2020), under a General Time Reversible model (GTR+G) based on the Bayesian Information Criterion from a model testing analysis performed in MEGA7 (Kumar *et al.* 2016) and testing node support with 500 full non-parametric bootstrap replicates. Sequences of *Geckolepis* spp. (GenBank accessions JQ974310 / AB661666) were used as outgroup. Uncorrected pairwise genetic distances were calculated from the 16S and ND4 sequences using MEGA7.

The alignments of the nuclear-encoded fragments of the RAG-1 and CMOS genes were analyzed independently to understand concordance (or absence thereof) in their differentiation. We used a genealogy visualization approach to graphically represent the relationship among alleles (haplotypes). Haplotypes were estimated with the PHASE algorithm (Stephens *et al.* 2001), and a haplotype network using the TCS algorithm (Templeton *et al.* 1992; Clement *et al.* 2000) was constructed in Hapsolutely (part of iTaxoTools) (Vences *et al.* 2021, 2024a).

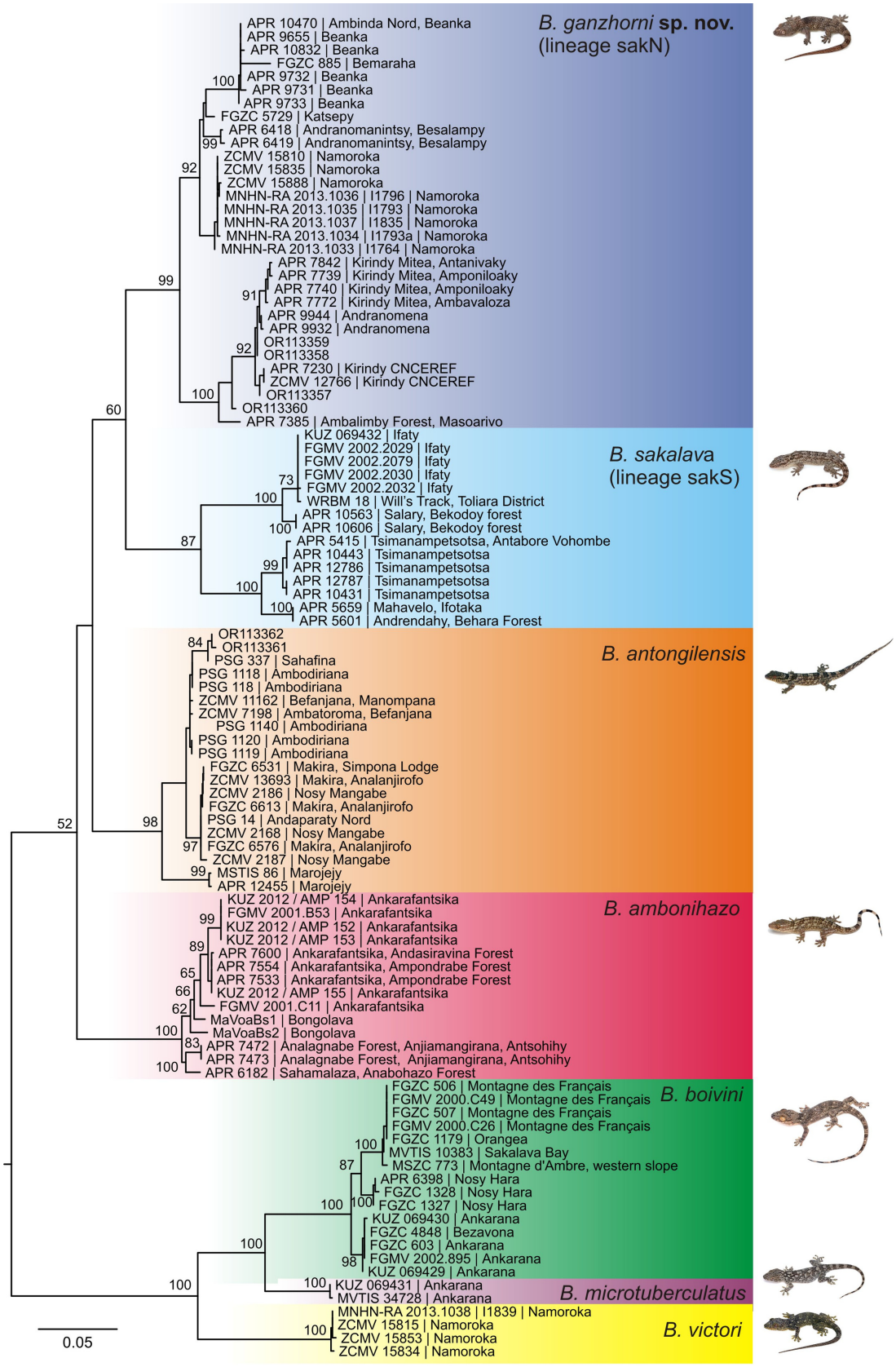

FIGURE 2. Maximum Likelihood tree based on a 1764 bp alignment of the mitochondrial ND4 gene of available sequences of *Blaesodactylus*. Terminals note the collection number or GenBank accession number, followed by the locality in Madagascar (as far as reliably available). Values at nodes are bootstrap proportions in percent (500 replicates; not shown if <50%). A sequence of *Geckolepis* was used as the outgroup (graphically removed post-analysis for simplification). Inset pictures show representative individuals of the respective species as in Fig. 1.

To delimit species, we follow the general lineage concept (de Queiroz 1998, 2007) but demanding a "soft" biological species criterion to be fulfilled: reproductive isolation, i.e., restricted gene flow among lineages (as e.g., Speybroeck *et al.* 2020). As a proxy for ascertaining this condition, we apply a genealogical concordance species criterion (Avise & Ball 1990) between mitochondrial and nuclear loci, especially in populations occurring in sympatry or close geographical proximity (see also Avise & Wollenberg 1997), along with concordance between genetic and morphological evidence (Padial *et al.* 2010; Miralles *et al*. 2024). We here use the term "lineage" to refer to genealogical lineages at or below the species level, and "clade" to refer to monophyletic groups with reference to a phylogenetic tree (see also Vences *et al.* 2024b for more details about this terminology).

Results

Phylogeny and molecular differentiation

The ML tree inferred from a 1764 bp ND4 + 12S + 16S alignment comprising 101 samples of *Blaesodactylus* (Fig. 2) reconstructs all currently accepted species as monophyletic groups. As in previous studies based on only ND4 (Bauer *et al.* 2011; Jono *et al.* 2015; Ineich *et al.* 2016), most of the deep phylogenetic relationships among species-level lineages are not reliably reconstructed, as is recognizable from poor bootstrap support of the respective nodes. Among the well-supported relationships, *B. microtuberculatus* was found sister to the syntopic *B. boivini* (bootstrap support BS = 100%), and the clade containing these two species was sister to *B. victori* (BS = 100%; see also Ineich *et al.* 2016). Samples of populations currently assigned to *B. sakalava* fell into two main clades, one geographically found in the South and South West of Madagascar (reaching northwards up to Salary-Bekodoy, ca 22.5°S, at its northernmost extent; BS = 87%; here named lineage sakS; Figs. 2–3), and one in the West and North West regions (reaching southwards until Kirindy Mitea, ca 20.8°S, at its southernmost extent; BS = 99%; here named lineage sakN; Figs. 2–3); the clade containing sakS and sakN, herein referred to as the *B. sakalava* complex, was only weakly supported (BS = 60%). Each of the two main lineages of the *B. sakalava* complex, sakS and sakN, contained two further phylogeographic clades: within lineage sakN, sequences from the northernmost localities Beanka, Bemaraha, Besalampy, Katsepy and Namoroka (BS = 92%) were sister to sequences from Ambalimby, Ambinda, Andranomena, Kirindy, and Kirindy Mitea (BS = 100%). And within lineage sakS, sequences from the southernmost sites Andrendahy, Mahavelo-Ifotaka, and Tsimanampetsotsa (BS = 100%) were sister to those from Ifaty, Salary-Bekodoy, and an unspecified locality corresponding to a sequence from GenBank from "Will's Track" in Toliara (BS = 100%) (Fig. 3).

Uncorrected pairwise divergences in the ND4 fragment between lineages ranged between a minimum of 9.8% between *B. ambonihazo* and *B. antongilensis*, and a maximum of 21.5% between *B. sakalava* (lineage sakS) and *B. microtuberculatus* (Table 1). Sequences of lineages sakN vs. sakS differed by 12.1–15.3%, and within these two lineages, divergences up to 8.5% (sakN) and 10.5% (sakS) were identified. Uncorrected pairwise distances in the 16S fragment ranged from 4.7% (*B. microtuberculatus* vs. *B. boivini*) to 13.4% (*B. microtuberculatus* vs. *B. sakalava* (lineage sakS) and amounted to 8.4–8.5% between lineages sakN and sakS (Table 1).

The RAG-1 haplotype network (Fig. 4) is based on an alignment of 302 bp for 140 sequences after phasing (thus, from 70 samples). Similar to previous RAG-1 data (Bauer *et al.* 2011; Ineich *et al.* 2016) a phylogroup containing all sequences of *B. boivini* (two haplotypes) and *B. victori* (one haplotype) was separated by 5–6 and 3 mutational steps, respectively, from the other species. The single haplotype containing all sequences of *B. ambonihazo* differs by one mutational step from the central haplotype that is shared among *B. antongilensis* and lineages sakS and sakN. The CMOS haplotype network (Fig. 4) is based on an alignment of 437 bp for 122 sequences after phasing (thus, from 61 samples). Here, a central haplotype is shared by *B. ambonihazo*, *B. victori* and lineage sakN, whereas *B. antongilensis* and *B. microtuberculatus* sequences formed species-specific haplotypes differing by 1 and 2 mutational steps, respectively. Lineage sakS had 6 haplotypes, none of which was shared with sakN or any other *Blaesodactylus* species. The nuclear gene sequences also confirmed two further localities for the sakS lineage (Roy Benono and Tsingilo) and one locality for the sakN lineage (Antrema) for which no mitochondrial sequences could be obtained (Fig. 3)

TABLE 1. Uncorrected pairwise distances (in %) among fragments of the mitochondrial genes for ND4 (under the diagonal) and 16S rRNA (above the diagonal). Shown is the minimum and maximum in pairwise comparisons. Note that values are less variable for the 16S comparisons as these are based only on 1–2 individuals per species. Values in italics are intraspecific comparisons for ND4 and 16S, respectively.

◣ ND4 ◥ 16S	*B. ambonihazo*	*B. antongilensis*	*B. boivini*	*B. microtub.*	*B. ganzhorni* **sp. nov.**	*B. sakalava*	*B. victori*
B. ambonihazo	*0.0–4.1 / 1.5*	8.1–8.8	11.6–13.1	11.6–12.4	7.3–7.9	7.3–8.4	11.4–11.9
B. antongilensis	9.8–11.5	*0.0–5.3 / 0.0*	11.8–11.8	11.1	7.1	9.2–9.4	11.0
B. boivini	16.8–18.8	16.6–18.8	*0.0–3.4 / 0.8*	4.7	11.2–11.6	12.9–13.2	7.2–8.0
B. microtub.	16.8–17.9	18.1–18.6	10.5–11.9	*0.0–0.0 / –*	11.2	13.3–13.4	7.4–7.6
B. ganzhorni **sp. nov.**	11.9–16.2	11.1–14.9	16.8–19.4	16.9–19.4	*0.0–8.5 / 0.0*	8.4–8.5	10.4
B. salalava	14.7–16.9	13.0–16.6	17.7–21.1	20.9–21.5	12.1–15.3	*0.0–10.5 / 0.0*	12.1–12.3
B. victori	15.3–16.9	16.4–17.3	15.6–16.8	14.5–14.9	16.0–17.7	18.8–20.5	*0.0–0.4 / 0.4*

Geographical distribution

Samples studied and identified by molecular data herein (Figs. 2, 4) considerably extend the knowledge of the geographical ranges of various *Blaesodactylus* species (Fig. 3). We provide two new locations (Bongolava plateau, no precise coordinates available; and Analagnabe, 15.1567°S, 47.7350°E) for *B. ambonihazo*, both located inbetween the two known localities Ankarafantsika and Sahamalaza Peninsula (the latter reported by Penny *et al.* 2017 based on a COI sequence, GenBank accession number MG189479, and confirmed herein by a new sample). For the east coast species *B. antongilensis*, our molecular data confirm its occurrence in the Marojejy Massif which has recently been reported based on morphological identification (Rakotoarimalala & Raselimanana 2023). We here also report the occurrence of lineage sakN from Antrema and Katsepy (ZSM 232/2018 [FGZC 5729], 15.7625°S, 46.2436°S, 9 m a.s.l.), extending the distribution of the *B. sakalava* complex ca. 120 km northeastwards from Namoroka (Fig. 3) which so far was the northernmost record confirmed by molecular data (Ineich *et al.* 2016). For lineage sakS, our data confirm its occurrence at two sites (Mahavelo-Ifotaka and Andrendahy) which are close to the southeastern limits of the southern spiny thornbush biome. Finally, our record of *B. boivini* from Bezavona (ZSM 1503/2012 [FGZC 4848], ca. 13.52°S, 49.83°E; Fig. 3) extends the confirmed distribution of this species southeastwards, and a further record of this species from the western slope of Montagne d'Ambre at 804 m above sea level (specimen MSZC 773; geographical coordinates 12.5844°S, 49.1149°E) might be the highest elevational record for *Blaesodactylus*. The additional samples sequenced for *B. microtuberculatus* and *B. victori* confirm the genetic identity of these apparent karst specialists, respectively endemic to the Ankarana and Namoroka limestone massifs.

Morphological divergence

Despite overall morphological similarity of specimens assigned to lineages sakN and sakS, detailed morphological examination revealed several differences between them.

Comparison of color patterns reveals substantial variation between individuals, but these differences can be attributed to individual variation rather than differences between lineages. Some specimens both of sakS (Fig. 1, 5B) and sakN (Fig. 6C) show a longitudinal arrangement of dorsal dark markings forming irregular and interrupted stripes which is absent in other specimens of both lineages (Fig. 5, 6). Also, specimens active during the day (e.g., Fig. 6B, G, H) often show a much darker color with less distinct pattern than those active at night (e.g., Fig. 6A), which blurs the detection of possible chromatic differences between the two lineages. While the original tail in both lineages has a pattern of alternating horizontal dark and light bands, the regenerated tails have indistinct longitudinal dark and light lines and vermiculations. One juvenile of lineage sakN (Fig. 6F) had a conspicuous yellowish color on the ventral side which was also observed in several adults from this site.

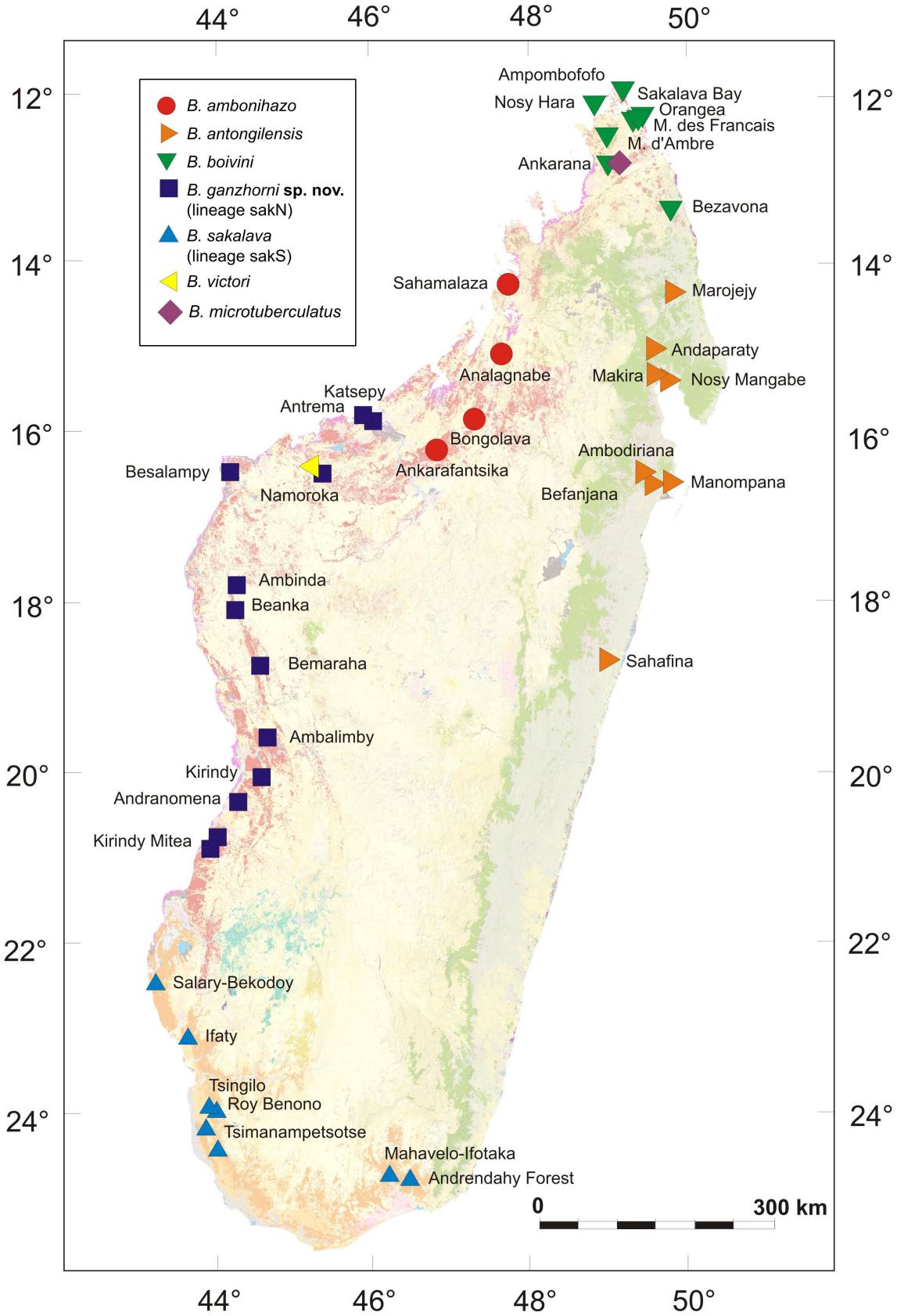

FIGURE 3. Map of Madagascar showing localities of all the seven recognized species of *Blaesodactylus* verified by DNA sequence analysis. The base map shows vegetation across Madagascar from the Madagascar Vegetation Mapping Project (Moat & Smith 2007; available at https://web.archive.org/web/20180419112513/http://www.vegmad.org/). Vegetation is colored as follows: green, humid forest (rainforest); red, western dry deciduous forest; pink, mangroves; orange, spiny forest-thicket; greenish blue, western subhumid forest.

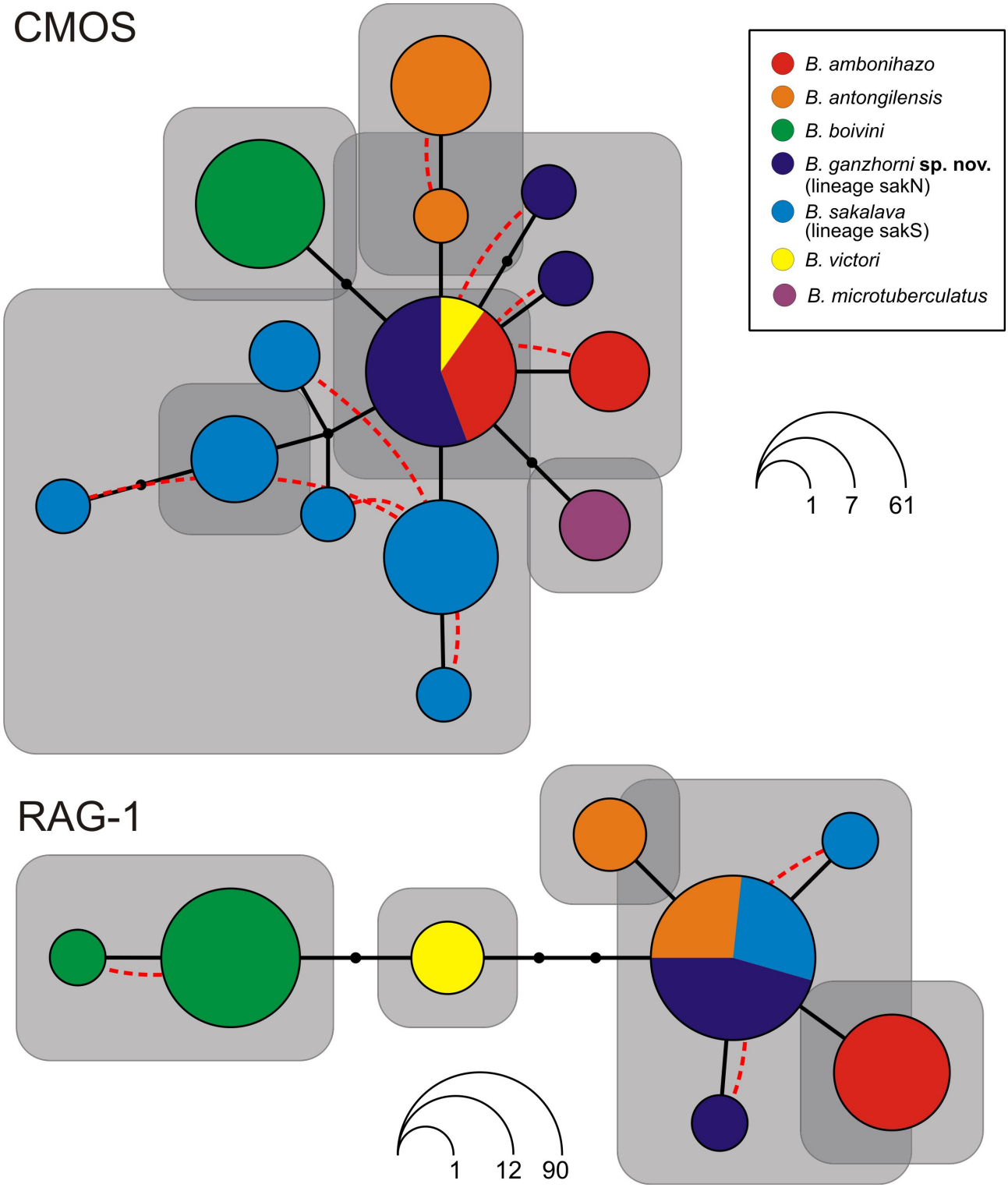

FIGURE 4. Haplotype networks of nuclear-encoded fragments of the genes for CMOS (437 bp, 61 samples) and RAG-1 (302 bp, 70 samples) and CMOS (437 bp, 61 samples) of *Blaesodactylus*. Sequences were phased before network reconstruction. Small black dots represent unsampled hypothetical alleles that each correspond to an additional mutational step. Red dashed curves represent connections between distinct haplotypes found co-occurring in heterozygous individuals. Gray rectangles indicate fields for recombination.

Three meristic characters could only be verified in a limited number of specimens (sakN, N=3; sakS, N=4; Table 2) and therefore require confirmation by future studies. The lineage sakN probably has higher longitudinal

counts of dorsal and ventral scales, but these values overlap in the two lineages (LCDS 428–452 vs. 394–430; LCVS 185–213 vs. 173–189) (Table 2). Furthermore, it is possible that specimens of sakN have a relatively longer head (HW/SED 0.65–0.84 vs. 0.87–0.95; Table 2, Fig. 7),

One character distinguishing most specimens of the two lineages but difficult to quantify by measurements or counts is the distinctness of dorsal and lateral tubercles, which are less expressed in sakN. This is particularly obvious laterally on the head, with no or only small tubercles visible above the ear in most specimens of sakN whereas in sakS, there are usually several distinct tubercles clearly visible above the ear (see Fig. 5). This character was verified by examination of vouchers or from photographs of non collected specimens, in at least 13 specimens of sakN and seven specimens of sakS

The most clearly diagnostic character is the longer postmental scales relative to the width of mental scale in sakS. To verify the variation in this character, we calculated the ratio of mental width vs. postmental length in 11 sakN and seven sakS specimens and found a clear separation without overlap (ratio postmental length / mental width 0.61–0.69 in sakN and 0.78–0.90 in sakS; Fig. 8 and raw data available at https://doi.org/10.5281/zenodo.14889416). This difference was statistically highly significant (Wilcoxon-Mann-Whitney U test, Z = -3.487, P = 0.0005).

Species delimitation in the *Blaesodactylus sakalava* complex

Our data set contains a substantial amount of new data on the molecular variation of *Blaesodactylus* populations assigned to *B. sakalava* from across its entire range. The mitochondrial tree (Fig. 2) separates two highly supported lineages, sakN and sakS, within the *B. sakalava* complex, corresponding to populations occurring roughly north vs. south of Morombe (roughly south of Mangoky river). The amount of mitochondrial divergence among these two lineages (12.1–15.3% in ND4; 8.4–8.5% in 16S) is higher than that found between closely related but clearly distinct species of *Blaesodactylus*, such as *B. boivini* and *B. microtuberculatus* (10.5–11.9 % in ND4; 4.7% in 16S) (Table 1). Furthermore, sakN and sakS are also fully separated in the nuclear-encoded CMOS DNA fragment, lacking any haplotype sharing between them (Fig. 4). Furthermore, there are probable differences in relative head length and scale counts of dorsal and ventral side, clearly perceptible differences in the expression of dorsal and lateral tubercles, and very obvious differences in the longitudinal extension of postmental scales.

Based on high mitochondrial divergence, concordant with differentiation in one nuclear-encoded gene and several independent morphological characters, we conclude that the two lineages of the *B. sakalava* complex, sakN and sakS, should be considered evolutionarily independent lineages, meriting a status as distinct species. Based on the geographic provenance of the name-bearing types of *B. sakalava* and its junior synonym *Homopholis heterolepis* Boulenger, 1885, and the morphological characteristics of these specimens, both of these *nomina* are to be assigned to the southern sakS lineage (see section Taxonomy below for more detail). Therefore, lineage sakN is in the following named and described as a new species.

Taxonomy

As argued above, our data provide evidence for two distinct evolutionary lineages meriting species status and currently subsumed under the name *Blaesodactylus sakalava.* To translate this conclusion into a new classification requires reliably assigning two available *nomina* to these lineages: *Hemidactylus sakalava* Grandidier, 1867; and *Homopholis heterolepis* Boulenger, 1896.

Hemidactylus sakalava was described by Grandidier (1867) from "Tullear" (=Toliara), along with several other species of squamates from the South-West of Madagascar. According to Ineich *et al.* (2016), the nomen is based on two syntypes: MNHN-RA 0.5911 and MNHN-RA 1994.0417 (formerly MNHN-RA 5911A), both collected by A. Grandidier and registered in the MNHN collection in 1869. Morphological examination of both syntypes revealed typical morphological character states of the southern lineage: relatively short postmental scales and distinct tubercles above the ear opening. Along with the unambiguous provenance information, this provides conclusive evidence for assigning the nomen *sakalava* to lineage sakS.

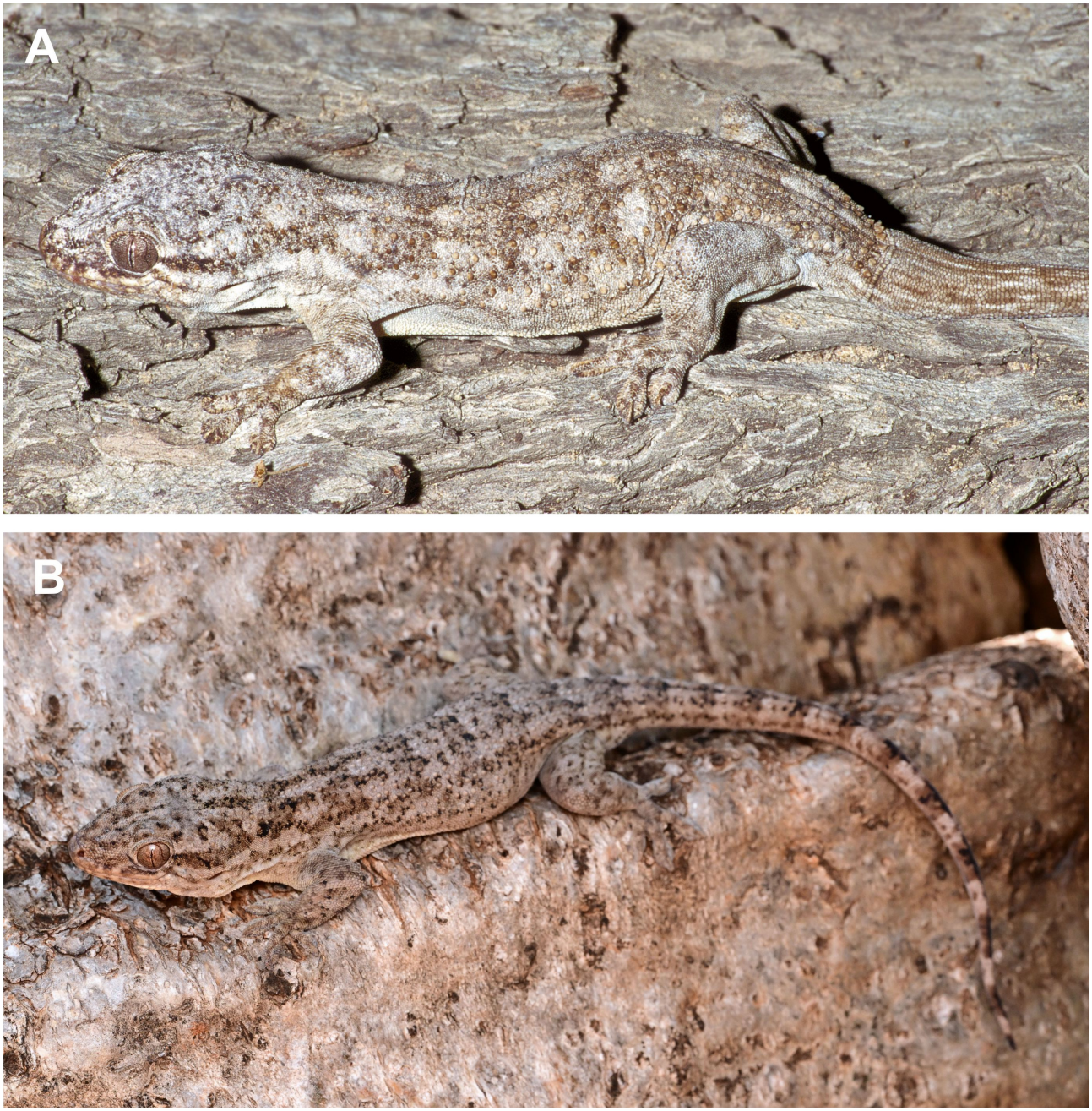

FIGURE 5. Specimens of *Blaesodactylus sakalava* sensu stricto in life. A, Specimen of from Ifaty (ZSM 589/2000). B, Specimen from Berenty (not collected).

Homopholis heterolepis was described by Boulenger (1896) from "a single female specimen" collected in "south-western Madagascar". The holotype apparently corresponds to BMNH (current acronym NHMUK) 1946.8.26.5 according to Russell (1978). A photograph of this specimen was reproduced by Böhme & Meier (1980), and Russell (1978) provides a drawing of the "chinshield pattern" which clearly shows the presence of rather short postmental scales. Along with the provenance "south-western Madagascar", this strongly suggests that also the nomen *heterolepis* is to be assigned to lineage sakS, and therefore its current status as junior synonym of *B. sakalava* sensu stricto is to be maintained.

Consequently, no earlier name is available for the lineage sakN which therefore is here described as a new species.

***Blaesodactylus ganzhorni* sp. nov.**
Figs. 1, 6–9.

Holotype. ZSM 106/2006 (field number FGZC 885), adult male with everted hemipenes, collected by F. Glaw, J. Köhler, P. Bora and H. Enting on 26 March 2006 in Bendrao Forest ("Camp 3", geographical coordinates 18.7844° S, 44.8603° E, 427 m a.s.l.), Tsingy de Bemaraha National Park, Madagascar.

Paratypes. A total of ten specimens, all from western Madagascar. ZSM 825/2010 (ZCMV 12766), collected by A. Miralles and A. Rakotoarison on 4 December 2010 in the Kirindy reserve CNCEREF (base camp; 20.0674° S, 44.6569° E, 55 m a.s.l.); ZSM 232/2018 (FGZC 5729), adult male with everted hemipenes, collected by F. Glaw, D. Prötzel, N.A. Raharinoro, R.N. Ravelojaona, A. Razafimanantsoa, J. Forster, K. Glaw, T. Glaw & C. Zanotelli on 31 March 2018 in Katsepy, garden of hotel "Madame Chabaud" (15.7624° S, 46.2436° E, 9 m a.s.l.); ZSM 62/2023 (ZCMV 15810), collected at Tsingy de Namoroka, by A. Miralles, N. A. Rahagalala, A. Rakotoarison, D. Razafimanafo & A. Razafimanantsoa on 7 October 2023 at Tsingy de Namoroka (Campsite 1, east of Tsingy massif, near a small temporary lake, 16.4310° S 45.3661° E, 120 m a.a.l.); ZSM 86/2023 (ZCMV 15835), collected by A. Miralles, N. A. Rahagalala, A. Rakotoarison, D. Razafimanafo & A. Razafimanantsoa between 17:00 and 19:00 on 8 October 2023 at Namoroka (Petit Tsingy, east of Tsingy massif, 16.4354° S, 45.3684° E, 124 m a.s.l.); UADBA-ZCMV 15888, collected by A. Miralles, N. A. Rahagalala, A. Rakotoarison, D. Razafimanafo & A. Razafimanantsoa between 19:00 and 22:00 on 11 October 2023 at Namoroka (Vicinity of Camp 2: Grand Tsingy, south of the Tsingy massif, 16.4697° S, 45.3467° E, 135 m a.sl.); MNHN-RA 2013.1033 (I1764), collected by I. Ineich on 3 September 2012 at the Tsingy de Namoroka (16.4706° S, 45.4087° E, 139 m a.s.l.); MNHN-RA 2013.1034 (I1793b), collected by I. Ineich on 3 September 2012 at the Tsingy de Namoroka (16.4657 °S, 45.3531° E, 124 m a.s.l.); MNHN-RA 2013.1035 (I1793w), collected by I. Ineich on 8 September 2012 at the Tsingy de Namoroka (ca. 16.470° S, 45.336° E, ca. 125 m a.s.l.); MNHN-RA 2013.1036 (I1796), collected by I. Ineich on 3 September 2012 at the Tsingy de Namoroka (ca. 16.45° S, 45.35° E, ca. 145 m a.s.l.); MNHN-RA 2013.1037 (I1835), collected by I. Ineich on 10 September 2012 at the Tsingy de Namoroka (16.4675° S, 45.3594° E, 129 m a.s.l.).

Additional material. Four additional voucher specimens are assigned to the new species but not included in the paratype series due to the lack of molecular identification: MNHN-RA 2016.0053 (I1261), collected by I. Ineich on 23 October 2016 at the Tsingy de Namoroka (16.40° S, 45.30° E, ca. 122 m a.s.l.); MNHN-RA 2016.0051 and MNHN-RA 2016.0052 (respectively I1406 and I1420), collected by I. Ineich on 29 October 2016 at the Tsingy de Namoroka (no GPS readings available); UABDA-ZCMV 12712 collected by A. Miralles & A. Rakotoarison on 29 November 2010 in the Kirindy reserve CNCEREF (no exact locality); ZSM 826/2010 (ZCMV 12750), collected by A. Miralles & A. Rakotoarison on 3 December 2010 in the Kirindy reserve CNCEREF (Sentier des Pandanus; 20.0763° S, 44.6748° E, 57 m a.s.l.).

Diagnosis. Assigned to the genus *Blaesodactylus* based on large body size (SVL up to 113 mm; MNHN-RA 2013.1035), undivided lamellae under fingers and toes, dorsal skin made up of small granular scales with intermittent, regularly spaced enlarged conical tubercles, and molecular phylogenetic relationships. Within the genus, *B. ganzhorni* **sp. nov.** is distinguished from *B. ambonihazo* by mostly having a grayish dorsal coloration in life, with poorly contrasted dark gray markings (vs. more contrasted, often brownish dorsal color, with dark brown color especially on tail crossbands); from *B. antongilensis* by grayish dorsal coloration with poorly contrasted dark gray markings (vs. more contrasted, often brownish dorsal color, with dark brown color especially on tail crossbands); from *B. boivini* by smaller body size (maximum recorded SVL 113 mm vs. 144 mm), less strongly expressed tubercles especially on the sides of the head and above the ear (vs. usually distinct tubercles present on side of the head and above ear), weakly expressed whorls of tubercles over full length of original tail (vs. pairs of tubercles on proximal third of tail) and a nostril usually not colored black inside (vs. nostrils black); from *B. microtuberculatus* by presence of prominent and at least partially and weakly keeled enlarged dorsal tubercles (vs. flattened, unkeeled and very inconspicuous), presence of caudal tubercles (vs. absence), uniformly pale gular region (vs. mottled), and a nostril not colored black (vs. nostrils black); and from *B. victori* by presence of prominent and at least partially and weakly keeled enlarged dorsal tubercles (vs. flattened and unkeeled), presence of caudal tubercles (vs. absence), absence of dorsal whitish circular spots (vs. presence), and a nostril not colored black (vs. nostrils black). [note that in rare cases the color of nostrils refers to the inner skin/mucosa surrounding the nostril opening and differences may not be obvious in preserved specimens, perhaps depending on the state of fixation].

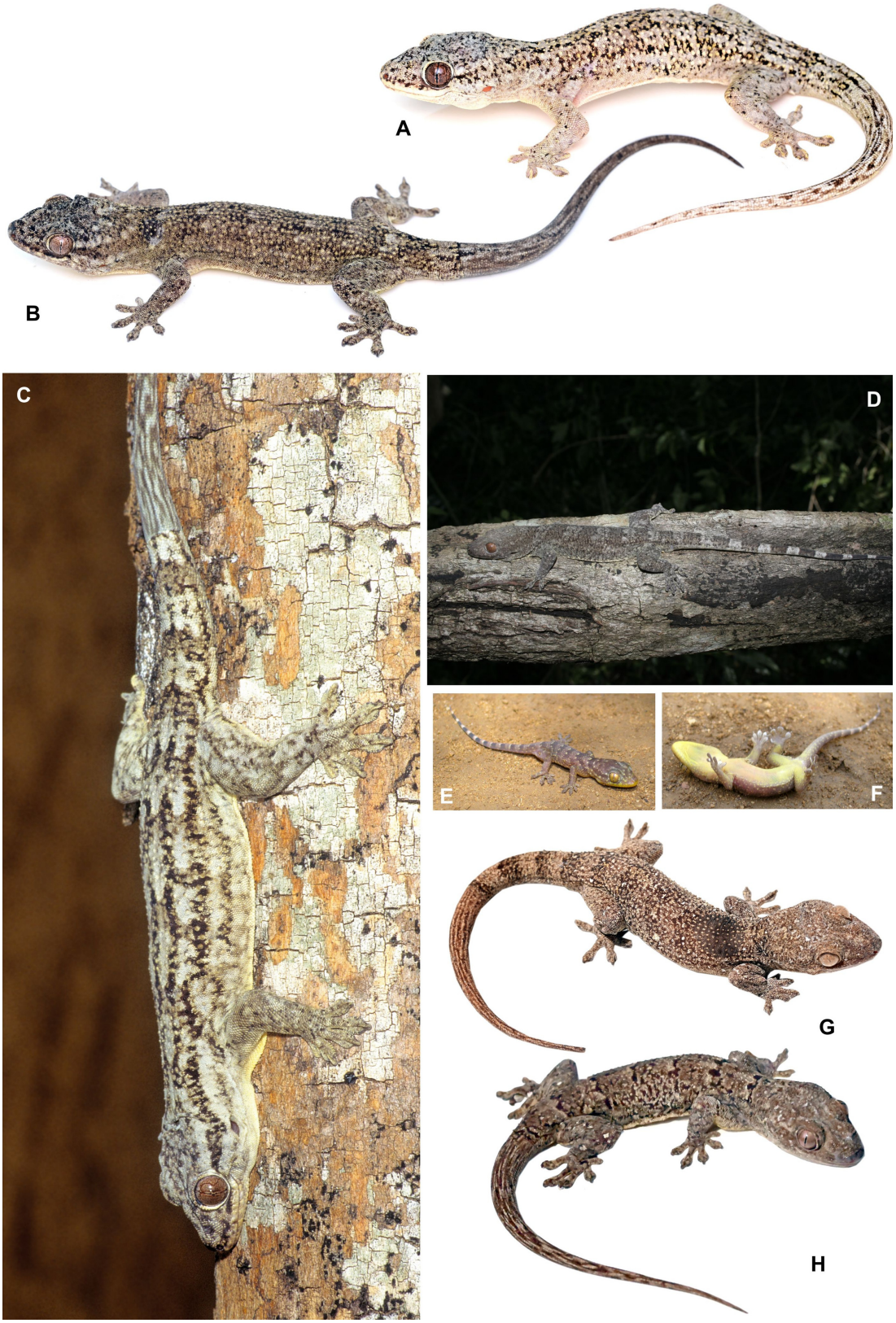

FIGURE 6. Specimens of *Blaesodactylus ganzhorni* **sp. nov.** in life. A, Specimen from Kirindy in night coloration (not collected; photographed November 2024). B, Specimen from Akiba south of Kirindy in day coloration (not collected; photographed November 2024). C, Specimen from Kirindy (not collected, photographed in 1995). D, Specimen from the Tsingy de Bemaraha (holotype, ZSM 106/2006). E, F, Juvenile specimen from Kirindy, probably corresponding to ZSM 826/2010 (ZCMV 12750). G, Paratype of *B. ganzhorni* **sp. nov.** from Namoroka, ZSM 62/2023 (ZCMV 15810). H, Paratype of *B. ganzhorni* **sp. nov.** from Namoroka, UADBA-ZCMV 15888.

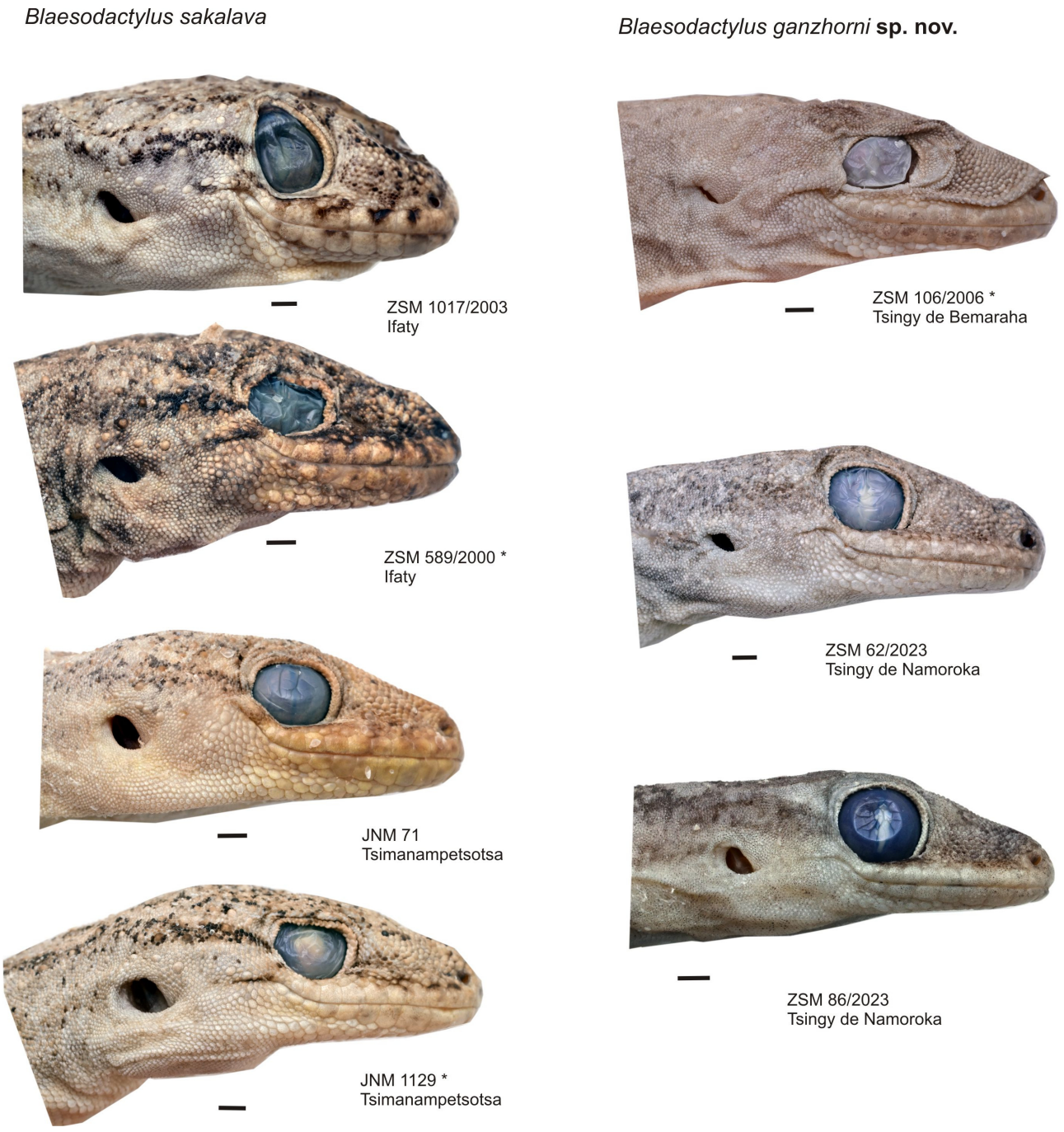

FIGURE 7. Comparative lateral views of head of representative preserved specimens of *Blaesodactylus sakalava* and *B. ganzhorni* **sp. nov.** Note the more strongly expressed dorsal and lateral tubercles in *B. sakalava* where most specimens have a series of 3–4 distinct tubercles above the ear opening which are much smaller or missing in *B. ganzhorni* **sp. nov**. Scale bars = 2 mm.

The new species is most similar to its sister species, *B. sakalava*, but differs from it morphologically by a relatively longer head (HW/SED 0.65–0.84 vs. 0.87–0.95; Table 2), relatively longer postmentals scales relative to width of mental scale (ratio mental width vs. postmental length 0.61–0.67 vs. 0.78–0.90), less expressed tubercles on the dorsum and especially laterally on head, with no or only small tubercles visible above the ear in most specimens (vs. more distinct tubercles, usually several distinct tubercles visible above ear, see Fig.6), and probably larger longitudinal counts of dorsal and ventral scales, despite overlap in these values (LCDS 428–452 vs. 394–430; LCVS 185–213 vs. 173–189; Table 2).

TABLE 2. Morphometric and meristic data of selected specimens of *Blaesodactylus ganzhorni* **sp. nov.** (HT, holotype; PT, paratypes) and *B. sakalava* (ST, syntype). Measurements of MNHN specimens taken from Ineich *et al.* (2016) and measured by I. Ineich; for additional measurements of these specimens, see Ineich *et al.* (2016). NM, not measured. * measured to the nearest 0.5 mm ** broken tail, *** regenerated tail.

Specimen voucher	Field number	Locality	Sex	Type status	SVL (mm)	TAL (mm)	HIL (mm)	HW (mm)	SED (mm)	HW/SED	**ED (mm)**	**SUPL**	**INFL**	**LongTub**	**LCDS**	**LCVS**
B. ganzhorni **sp. nov.** (lineage sakN)																
ZSM 106/2006	FGZC 885	Bemaraha	M	HT	103.0	138	39.0	21.8	25.9	0.84	5.8	12	11	59	452	213
ZSM 62/2023	ZCMV 15810	Namoroka	M	PT	100.7	123.8***	44.4	21.4	25.4	0.84	6.0	10	8–9	51	436	193
ZSM 825/2010	ZCMV 12766	Kirindy	F?	PT	92.6	91.6***	35.0	20.4	31.2	0.65	5.7	10	11	57	428	185
MNHN 2013.1033	I1764	Namoroka	F	PT	102*	117*	NM	27.5	NM	NM	6.5	11/12	9/11	NM	NM	NM
MNHN 2013.1034	I1793b	Namoroka	F	PT	103*	121*	NM	25.5	NM	NM	6.2	11/12	10/10	NM	NM	NM
MNHN 2013.1035	I1793w	Namoroka	M	PT	113*	106*	NM	29.2	NM	NM	7.3	14/12	10/10	NM	NM	NM
MNHN 2013.1036	I1796	Namoroka	SA	PT	63*	84*	NM	17.6	NM	NM	4.9	12/13	10/9	NM	NM	NM
MNHN 2013.1037	I1835I	Namoroka	M	PT	86*	108*	NM	22.3	NM	NM	6.0	11/11	10/9	NM	NM	NM
B. sakalava (lineage sakS)																
ZSM uncatalogued	JN 1129	Tsimanam-petsotsa	F?	–	91.4	106.4***	36.1	20.6	21.7	0.95	4.6	10	10–11	56	404	173
ZSM uncatalogued	JN 1171	Tsimanam-petsotsa	M?	–	85.8	98.5	36.2	18.5	21.0	0.88	4.6	10	10–11	58	430	180
ZSM 589/2000	FGMV 2000.519	Ifaty	F?	–	103.7	70.2***	41.2	22.5	25.4	0.89	5.4	11	10	52	415	184
ZSM 1017/2003	FGMV 2002.2023	Ifaty	F?	–	102.9	102.8**	44.0	21.7	24.9	0.87	5.7	11	9–10	59	394	189
MNHN 5911		Southwest Madagascar		ST	98*	100***	NM	27.7	NM	NM	6.1	11	11	NM	NM	NM
MNHN 1994.417	5911A	Southwest Madagascar		ST	84.5*	NM**	NM	22.6	NM	NM	5.1	11	10	NM	NM	NM

Description of the holotype. ZSM 106/2006 (field number FGZC 885), adult male with fully everted hemipenes (Fig. 9) and original tail. Snout–vent length 103 mm, original tail length 138 mm, head relatively long (HeadL = 31.5 mm) and wide (HeadW = 21.8 mm), wider than neck; snout elongate (SnEye = 12.3 mm), longer than horizontal eye diameter (OrbD = 5.8 mm), internarial distance 3.9 mm; smallest interorbital distance 10.8 mm, distance from snout tip to ear 25.9 mm. Scales on snout and forehead small, granular, heterogeneous, larger than those on occipital region except for scattered conical tubercles (with 2–3 times size of adjacent scales); pupil vertical with crenelated margins; superciliaries forming a short fold with small spines at anterior and posterior margins. Ear opening obliquely, slit-like (EarL = 2.4 mm) on left side (hidden in a fold on right side); eye to ear distance (EyeEar = 9.4 mm) longer than diameter of eye; rostral rectangular, much wider (4.3 mm) than high (2.2 mm), with a median groove; one internasal scale; head scales on snout just posterior to the large scales small, forming an atypical fold that was already visible in life (Fig. 8) and runs from the eye along supralabials and nostrils. Rostral in contact with the first supralabials, supranasals, and one enlarged internasal; nostrils round, each surrounded by enlarged supranasal, rostral, first supralabial and three postnasals; mental pentagonal, wider (3.4 mm) than long (1.8 mm); median pair of postmentals elongated (3.8 mm long), each bordered anteromedially by mental, laterally in broad contact with other postmental along most of their entire length, bordered anterolaterally by first infralabial, laterally by second postmental, posteriorly by several very small chin granules; 12 (right) and 12 (left) supralabials on both sides, 11 infralabials on both sides. Body stout, with distinct ventrolateral folds. Dorsal scales on body smooth, granular to slightly conical and juxtaposed, with intermittent, regularly spaced, weakly keeled, enlarged conical tubercles (ca. 3 x size of granular scales) which form indistinct rows and are separated from each other by ca. 4–7 small granules; approximately 15 irregular rows of these enlarged tubercles across dorsum, counted at midbody from one side to the other. Number of dorsal tubercles in a longitudinal row from head to base of tail 59; number of dorsal scales along the body, from first scale after the internasals to the first scale row or whorl of the tail 452. Ventral scales much larger than dorsal scales, smooth, mostly hexagonal, juxtaposed. 42 scale rows across venter between ventrolateral folds; longitudinal count of the number of ventral scales from the mental scale to the cloaca 213; gular region with relatively homogeneous, smooth, rounded to oval scales, juxtaposed. No precloacal or femoral pores. Ventral scales of limbs similar to other ventral scales, dorsal surface of limbs without enlarged scales or tubercles. Hindlimbs short (39.0 mm) and robust. Digits on hands broadly dilated, distal portion of digits II–V free of pad, bearing a prominent recurved and uncolored claw partly sheathed between a pair of scales, distal portion of digit I not free of pad, claw minute and lying in a groove in the adhesive pad; number of broad lamellae beneath each digit (10–13–16–18–14 manus; 11–13–15–17–14 pes); most lamellae undivided; interdigital webbing weakly developed. Relative length of digits (manus): IV>III>V>II>I; (pes): IV>III>V>II>I. Original tail slender, dorsoventrally depressed, tapering to tip, distinctly longer than SVL. Tail base with 3 smooth cloacal spurs on each side, the most dorsal being the largest. Scales on dorsal surfaces of tail largely homogeneous, but with weakly developed whorls of distinctly enlarged, keeled tubercles, which are most distinct in the four anterior whorls. Midventral subcaudal scales transversely enlarged more than half of tail width. Hemipenes fully everted (length 11.5 mm), apex bilobed, surface of apical lobes slightly granular, lacking distinctive calyces.

In life, ground color of dorsal surfaces of head, body, limbs and anterior part of the tail grey-brown with fine darker mottling and interspersed whitish tubercles (Fig. 8). Dorsum with a series of five moderately distinct and poorly delimited light gray crossbars between insertion of forelimbs and hindlimbs, darker anteriorly and fading towards the flanks. Tail with nine light gray crossbands, alternating with 10 dark gray bands. The bands are poorly delimited anteriorly, but show increasingly sharper borders towards the tail tip. Iris almost uniformly copper in distant view, with one reddish vessel like vertical line posteriorly and numerous dense fine red reticulations. Tongue tip red. Ground color of ventral surfaces of throat, chest, venter, ventral surfaces of fore- and hindimbs and tail base cream yellowish. Fine brown mottling on the anterior part of the throat, on ventral surfaces of limbs and the tail and distinct brown marbling on each side of the venter. Hands and feet including the adhesive lamellae light gray-brown. In preservative, after 18 years in ethanol, the coloration is similar to that in life, but substantially faded. Light crossbands on the back have almost disappeared. Whitish tubercles are still distinct, especially on the posterior part of the back. Alternating crossbands on the tail are still distinct. Ventral ground color has faded to cream white, and the brown mottling on the throat and the marbling on each side of the venter have almost disappeared. Hemipenes are creamy white. Iris is gray.

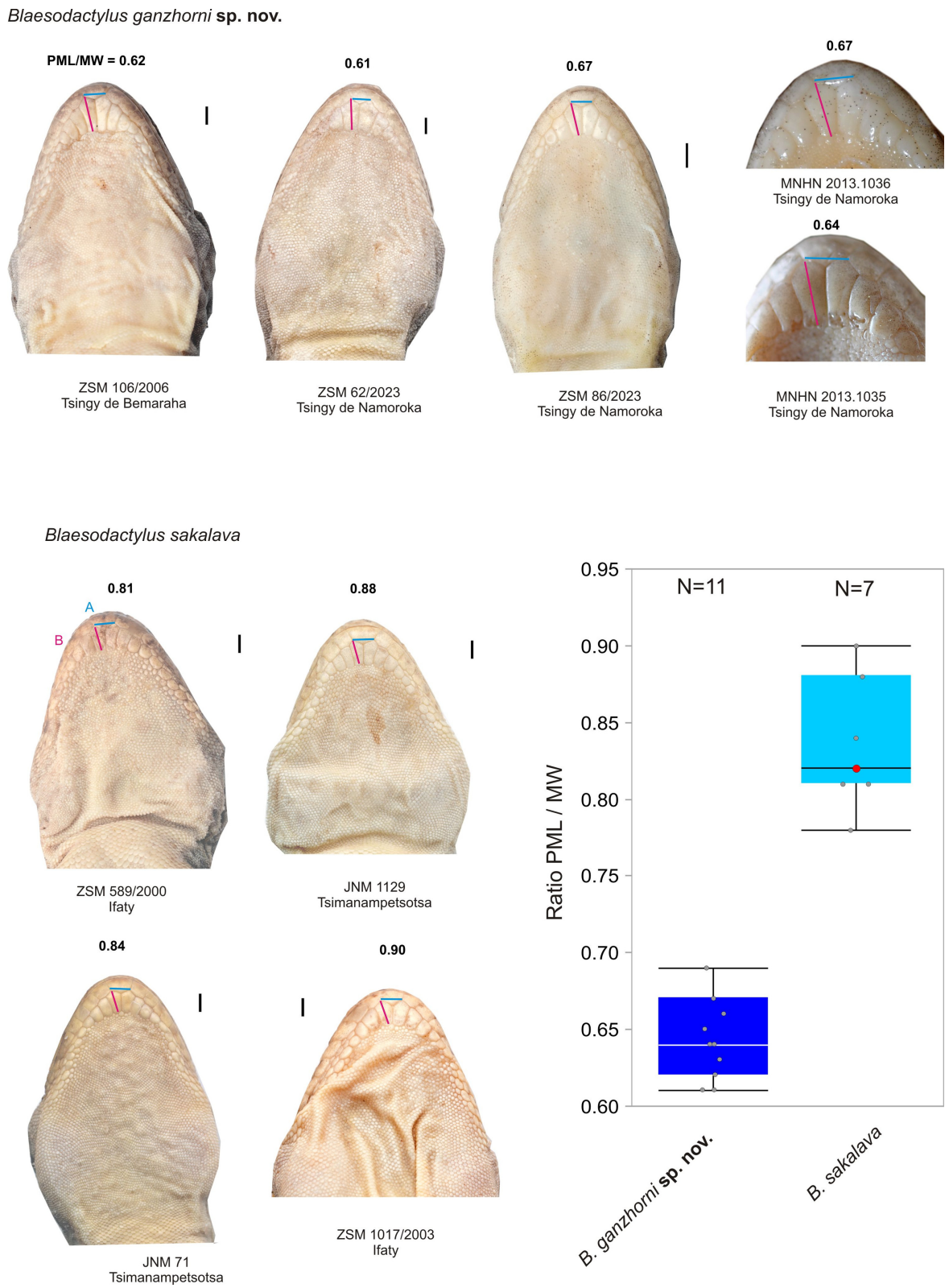

FIGURE 8. Comparative ventral views of head of representative preserved specimens of *Blaesodactylus sakalava* and *B. ganzhorni* **sp. nov.,** showing arrangement of scales in the gular region. Cyan and magenta lines mark the width of the mental scale at its posterior edge vs. the length of the central postmental scale; note the elongated shape of postmentals in *B. ganzhorni* sp. nov. which is reflected in lower values for the ratio of mental width / postmental length. Black scale bars = 2 mm. The inset graph is a boxplot of the values of this ratio in all specimens examined for these characters, showing minimum and maximum values as vertical line, 25% and 75% quantiles as box, median as horizontal line, single values as gray dots. The red dot is the value of the *B. sakalava* syntype MNHN-RA 5911.

FIGURE 9. Preserved male holotype of *Blaesodactylus ganzhorni* **sp. nov.**, ZSM 106/2006 (FGZC 885), from Bendrao, Tsingy de Bemaraha National Park, in dorsal (left) and ventral (right) views.

FIGURE 10. Habitat of *Blaesodactylus ganzhorni* **sp. nov.** in Kirindy reserve CNCEREF and Tsingy de Namoroka National Park. A, Dry forest at Kirindy. B, Landscape near the "Grand Tsingy" site in Namoroka. C, D, Periphery of the "tsingy" limestone area at Namoroka with baobab trees.

Variation: The paratypes are generally similar to the holotype in meristic variables and proportions (see Table 2 for additional details). The subadult paratype ZSM 86/2023 from Namoroka has a more contrasting coloration with very distinct crossbands on body and tail, but with a long uniformly light-colored tail tip (which is possibly regenerated). The juvenile paratype ZSM 826/2010 from Kirindy (not sequenced) has a brownish ground colouration in preservative with distinct crossbands on dorsum and tail. Another juvenile from Kirindy (ZCMV 12750), had a mallow-grayish overall dorsal coloration, marked with darker transverse bands and studded with many pale yellow small dots; a striking yellow coloration of the ventral side, particularly bright on the labial area; and a tail alternating dark gray and white rings, and whose color contrast is accentuated posteriorly (Fig. 8). ZSM 62/2023 (ZCMV 15810) from Namoroka bears an unusual wide, strikingly dark, almost black, patch on the dorsum. The fold of skin on the rostrum is apparently unique to the holotype, and almost certainly represents a malformation or an injury that may have originated during capture of the animal.

Etymology. The species name is an eponym, i.e., a noun in genitive case, dedicated to Jörg Ganzhorn, Hamburg University, in recognition of his enormous contributions to the research and conservation of Madagascar's biodiversity.

Natural history. A primarily nocturnal, but partially diurnal species. At Namoroka one specimen on 3 September 2012 was observed feeding during the day (sunny, without rain) with a prey in its mouth around 13:00 h, on a tree trunk about 1 m above the ground (MNHN-RA 2013.1033; a gravid female, with two eggs in abdominal cavity). The species can be found on tree trunks at 0.5–3 m above the ground, often in degraded dry deciduous forest (Fig. 10), often (as with other dry forest *Blaesodactylus*) in areas of baobab trees. During the day animals take refuge either in holes in tree trunks or in cavities on cave walls or stay on the trunk in shadow between two trunks, sometimes hiding under loose bark. Very often, they keep their heads or the entire body outside of their refuge during the day and

escape rapidly into the hole when feeling threatened or disturbed. In Kirindy, specimens have been found by night, at eye-level, on the trunks of medium-sized trees and on the wall of wooden cabins at the CNFEREF ecolodge. In Namoroka an individual was found at 0.5 m above the limestone, upside down at 20:45 h, suggesting that this species may hunt also on "tsingy" limestone rocks. Another specimen (ZCMV 15810) was spotted perched on a tree about 1 meter high in the small patch of forest surrounding the team's campsite (Camp 1). ZCMV 15835 was found nestled among the cliffs of the "Petit Tsingy" site at approximately 2 m high. ZCMV 15888 was observed perched in a tree near the grand Tsingy, also at a height of ca. 1 m. It also can be found near the ground on dead tree trunks. Several females were gravid when observed at Namoroka in September 2012 but not in October 2016.

Distribution. Known from arid western Madagascar, occurring approximatively between the two large rivers, Mangoky in the south and Betsiboka in the north (Fig. 3).

Discussion

This study provides the most comprehensive genetic survey of Madagascar velvet geckos to date, significantly extending the knowledge of the distribution ranges of several species. Because *Blaesodactylus* are large and prominent geckos that can easily be identified to genus, but on the other hand show only subtle morphological differences between species, there are numerous other locality records in the literature which however we have not revised here in detail. A full revision of all these sites would also be difficult due to the lack of photographs or voucher specimen information for many of them. The genetically verified records summarized in our map (Fig. 3) encompass the known distribution ranges of these species, although certainly many of these geckos occur at more sites in between those reported here. Madagascar velvet geckos include rather widespread species such as *B. antongilensis*, *B. ganzhorni* and *B. sakalava* whose known localities are spaced at maximum linear distances of approximately 520, 600 and 440 km, respectively, as well as local microendemics such as *B. microtuberculatus* and *B. victori* which apparently are restricted to single karstic massifs (see also Jono *et al.* 2015; Ineich *et al.* 2016). Although *Blaesodactylus* have colonized different biomes, i.e., southern spiny forest, western dry deciduous forest, as well as rainforest, all known locations are at relatively low elevations; the highest elevation record probably being that of *B. boivini* on the western slope of Montagne d'Ambre at 804 m above sea level. This site, however, is unusually arid for its elevation due to its position in the rain-shadow of Montagne d'Ambre and highly porous volcanic geology. Their overall distributional pattern suggests that *Blaesodactylus* have not been able to adapt to cool temperatures at higher elevations—a limitation they seem to share with the closely related Malagasy genus *Geckolepis*, but not with the related African *Homopholis*.

The two microendemic *Blaesodactylus*, *B. microtuberculatus* and *B. victori*, are both restricted to massifs consisting of eroded "tsingy" limestone, i.e., the Tsingy d'Ankarana and Tsingy de Namoroka, respectively. In at least two other gecko genera, *Lygodactylus* and *Paroedura*, tsingy specialists of cave- and rock-dwelling ecomorphs, and partly cave-dwelling habits, have evolved (Jackman *et al.* 2008; Glaw *et al.* 2014, 2018; Ineich & Bourgoin 2016; Vences *et al.* 2022b), and also the genera *Geckolepis*, *Phelsuma* and *Uroplatus* contain single microendemic species in Ankarana (Glaw *et al.* 2010; Lemme *et al.* 2013; Scherz *et al.* 2017; Ratsoavina *et al.* 2019). Although the large Tsingy de Bemaraha Massif holds some microendemic geckos such as *Paroedura spelaea*, *P. tanjaka* and *P. neglecta* (Glaw *et al.* 2018; Köhler *et al.* 2019) and *Lygodactylus hodikazo* (Vences *et al.* 2022b), and some further potential Bemaraha endemics still await detailed taxonomic revision (e.g., the *Phelsuma dubia* complex, see Rocha *et al.* 2009), it appears that overall fewer karst specialist gecko species have evolved there. In the case of *Blaesodactylus*, this might also be simply caused by a lack of biogeographic opportunity: the clade containing *B. boivini*, *B. microtuberculatus* and *B. victori* is only known to occur in the North and Northwest of Madagascar and may simply not have been able to disperse further southwards to reach the Tsingy de Bemaraha. As an alternative hypothesis, a karst-adapted *Blaesodactylus* species might still await its discovery in this extensive limestone massif.

In our phylogenetic tree, two *Blaesodactylus* specimens from the Marojejy Massif in the Northeast are confirmed to belong to *B. antongilensis*, as previously recorded by Rakotoarimalala & Raselimanana (2023) by morphological identification. This represents the northernmost reliably known locality for this species. Although the Marojejy specimens are sister to all other *B. antongilensis* in the mitochondrial tree (Fig. 2), their genetic distance to other *B. antongilensis* (up to 5.3% in ND4) is not impressively high. This conforms with the pattern observed in some other widespread geckos, *Paroedura gracilis* and *Phelsuma guttata*, where Marojejy, along with Andaparaty and

Nosy Mangabe, were also found to host genetically moderately divergent but likely conspecific lineages (Mohan *et al.* 2019). This pattern is not, however, universal among geckos; some are micro-endemic to Marojejy (e.g. *Lygodactylus ulli* in the subgenus *Domerguella*; Vences *et al.* 2022b), and for others Marojejy holds species with closer affinities to the North and Northeast regions, as opposed to the Northern Central East and Southern Central East regions (e.g. *Uroplatus giganteus*; Gehring *et al.* 2018).

Among the most conspicuous morphological differences between *Blaesodactylus* species are the weak expression of dorsal tubercles in the two microendemic species, *B. microtuberculatus* and *B. victori.* If the mitochondrial gene tree inferred here (Fig. 2) correctly reflects the species tree, then there is homoplasy in the size of dorsal tubercles: *B. boivini*, with strong tubercles similar to other species such as *B. sakalava*, is nested in a clade in which *B. microtuberculatus* and *B. victori*, both with very small tubercles, consecutively split off, with high bootstrap support. This suggests that either, *B. microtuberculatus* and *B. victori* have independently evolved a smoother dorsal integument, perhaps in the context of adaptation to living on karstic tsingy rocks (see above), or the strongly tubercular integument of *B. boivini* evolved or re-evolved independently from that of the other species, i.e., *B. ambonihazo*, *B. antongilensis*, *B. sakalava*, and *B. ganzhorni*.

Comprehensive assessments of genetic variation, phylogeography and taxonomy are crucial to determine conservation priorities and develop conservation management actions for widespread genera. In the case of *Blaesodactylus*, the present study only became possible by combining and studying tissue samples collected by various research teams and during multiple consecutive expeditions. Especially, materials collected during surveys by the Association Vahatra carried out in numerous remote sites in western and southern Madagascar (e.g., Raselimanana 2008) were of enormous value for elucidating the distribution of *B. ambonihazo*, *B. ganzhorni* and *B. sakalava.* This exemplifies the importance of continuous survey work, including the routine collection of voucher specimens and tissue samples (Nachman *et al.* 2023). Although our data do not support further taxonomic partitions within *B. sakalava* or *B. ganzhorni*, it is of relevance that each of these species consists of two distinct and geographically separate mitochondrial subclades. We did not detect, for these subclades, any differentiation between these in nuclear-encoded genes or in morphology, but we only analysed short nuclear gene fragments and had a very limited number of preserved voucher specimens available for examination (e.g., no preserved voucher of *B. sakalava* from the southernmost part of its range). Future studies should be carried out on additional voucher specimens and with more extensive genetic (ideally genomic) data sets, to investigate whether these mitochondrial subclades should be recognized as separate taxonomic units at the subspecies or even species level.

It is also of prime importance to survey the remaining remnants of primary habitat even if these are tiny and remote as any record from such relict sites can be crucial to fill gaps in our knowledge on distribution and phylogeography of the species encountered (e.g., Gehring *et al.* 2010). We reiterate that both funding bodies and permitting government agencies should continue to support and facilitate these activities to boost and refine science-based nature and reptile conservation in Madagascar (Kremen *et al.* 2008; Jenkins *et al.* 2014).

Acknowledgments

We are grateful to numerous colleagues, guides, field assistants, and students for their contributions during field expeditions, in particular to the late L. Allorge, J. Bezara, M. C. Bletz, P. Bora, T. Bourgoin, H. Enting, J. Forster, P. Galán, G. García, M. Gansuana, P.-S. Gehring, K. Glaw, T. Glaw, T. Haevermans, O. Hawlitschek, C. R. Hutter, J. Nopper, D. Prötzel, N. A. Rahagalala, N. A. Raharinoro, S. Rakotomanga, S. Rasamison, C. Rasoanaivo, F. M. Ratsoavina, R. N. Ravelojaona, A. Razafimanantsoa, and D. R. Vieites and C. Zanotelli. We are also indebted to L. Rothe and G. Keunecke for their contributions to the molecular laboratory work, and to M. Multzsch for assistance with taking morphometric and meristic measurements. Fieldwork was carried out in the framework of collaboration accords of the Technische Universität Braunschweig and the Zoologische Staatssammlung München with the Université d'Antananarivo, and the Ministry of the Environment, Water, Forests and Sustainable Development of the Republic of Madagascar. We thank the Malagasy authorities, in particular the "Direction des Aires Protégées, des Ressources Renouvelables et des Écosystèmes" and Madagascar National Parks, for research, collection, and export permits. The work of A.M. was funded by the Deutsche Forschungsgemeinschaft (grant MI 2748/1-1). The work of I.I. was supported through Labex funds. The work of M.D.S. and M.V. was funded by Deutsche Forschungsgemeinschaft (grant VE 247/13-1 and 15-1).

References

Arevalo, E., Davis, S.K. & Sites, J.W.Jr. (1994) Mitochondrial DNA sequence divergence and phylogenetic relationships among eight chromosome races of the *Sceloporus grammicus* complex (Phrynosomatidae) in Central Mexico. *Systematic Biology*, 43, 387–418.
https://doi.org/10.1093/sysbio/43.3.387

Avise, J.C. & Ball, R.M. (1990) Principles of genealogical concordance in species concepts and biological taxonomy. In: Futuyma, D. & Antonovics, J. (Eds.), *Oxford Surveys in Evolutionary Biology*. Oxford University Press, Oxford, pp. 45–67.
https://doi.org/10.1073/pnas.94.15.7748

Avise, J. & Wollenberg, K. (1997) Phylogenetics and the origin of species. *Proceedings of the National Academy of Sciences of the United States of America*, 94, 7748–7755.
https://doi.org/10.1073/pnas.94.15.7748

Bauer, A.M., Glaw, F., Gehring, P.-S. & Vences, M. (2011) New species of *Blaesodactylus* (Squamata: Gekkonidae) from Ankarafantsika National Park in north-western Madagascar. *Zootaxa*, 2942 (1), 57–68.
https://doi.org/10.11646/zootaxa.2942.1.2

Bauer, A.M., Scherz, M.D., Crottini, A., Ratsoavina, F.M. & Glaw, F. (2022) Gekkonidae, Geckos, Katsatsaka, TsaTsake. *In*: Goodman, S.M. (Ed.), *The New Natural History of Madagascar*. Princeton University Press, Princeton, New Jersey, pp. 1474–1479.
https://doi.org/10.2307/j.ctv2ks6tbb.211

Bell, J. (2008) A simple way to treat PCR products prior to sequencing using ExoSAP-IT. *Biotechniques*, 44, 834.
https://doi.org/10.2144/000112890

Böhme, W. & Meier, H. (1980) Revision der madagassischen *Homopholis* (*Blaesodactylus*)-Arten (Sauria: Gekkonidae). *Senckenbergiana Biologica*, 60, 303–315. [1979]

Boulenger, G.A. (1896) Descriptions of new lizards from Madagascar. *Annals and Magazine of Natural History*, Series 6, 17, 444–446.
https://doi.org/10.1080/00222939608680395

Boumans, L., Vieites, D.R., Glaw, F. & Vences, M. (2007) Geographical patterns of deep mitochondrial differentiation in widespread Malagasy reptiles. *Molecular Phylogenetics and Evolution*, 45, 822–839.
https://doi.org/10.1016/j.ympev.2007.05.028

Bruford, M.W., Hanotte, O., Brookfield, J.F.Y. & Burke, T. (1992) Single-locus and multilocus DNA fingerprint. *In*: Hoelzel, A.R. (Ed.), *Molecular Genetic Analysis of Populations: A Practical Approach*. IRL Press, Oxford, pp. 225–270.

Clement, M., Posada, D. & Crandall, K.A. (2000) TCS: a computer program to estimate gene genealogies. *Molecular Ecology*, 9, 1657–1659.
https://doi.org/10.1046/j.1365-294x.2000.01020.x

de Queiroz, K. (1998) The general lineage concept of species, species criteria, and the process of speciation. *In*: Howard, D.J. & Berlocher, S.H. (Eds.), *Endless Forms. Species and Speciation*. Oxford University Press, Oxford, pp. 49–89.

de Queiroz, K. (2007) Species concepts and species delimitation. *Systematic Biology*, 56, 879–886.
https://doi.org/10.1080/10635150701701083

Duméril, A.H.A. (1856) Description des reptiles nouveaux ou imparfaitement connus de la collection du Muséum d'Histoire Naturelle et remarques sur la classification et les caractères des reptiles. *Archives du Muséum d'Histoire Naturelle de Paris*, 8, 438–588.

Edler, D., Klein, J., Antonelli, A. & Silvestro, D. (2020) raxmlGUI 2.0: A graphical interface and toolkit for phylogenetic analyses using RAxML. *Methods in Ecology and Evolution*, 12, 373–377.
https://doi.org/10.1111/2041-210X.13512

Gehring, P.S., Ratsoavina, F.M. & Vences, M. (2010) Filling the gaps – amphibian and reptile records from lowland rainforests in eastern Madagascar. *Salamandra*, 46, 214–234.

Gehring, P.S., Siarabi, S., Scherz, M.D., Ratsoavina, F.M., Rakotoarison, A., Glaw, F. & Vences, M. (2018) Genetic differentiation and species status of the large-bodied leaf-tailed geckos *Uroplatus fimbriatus* and *U. giganteus*. *Salamandra*, 54, 132–146.

Glaw, F., Gehring, P.-S., Köhler, J., Franzen, M. & Vences, M. (2010) A new dwarf species of day gecko, genus *Phelsuma*, from the Ankarana pinnacle karst in northern Madagascar. *Salamandra*, 46, 83–92.

Glaw, F., Köhler, J. & Vences, M. (2018) Three new species of nocturnal geckos of the *Paroedura oviceps* clade from xeric environments of Madagascar (Squamata: Gekkonidae). *Zootaxa*, 4433 (2), 305–324.
https://doi.org/10.11646/zootaxa.4433.2.4

Glaw, F., Rösler, H., Ineich, I., Gehring, P.-S., Köhler, J. & Vences, M. (2014) A new species of nocturnal gecko (*Paroedura*) from karstic limestone in northern Madagascar. *Zoosystematics and Evolution*, 90, 249–259.
https://doi.org/10.3897/zse.90.8705

Grandidier, A. (1867) Liste des reptiles nouveaux découverts, en 1866, sur la côte sud-ouest de Madagascar. *Revue et Magazine de Zoologie, Paris*, Série 2, 19, 232–234

Greenbaum, E., Jackman, T. & Bauer, A.M. (2007) *Homopholis* and *Blaesodactylus* (Squamata: Gekkonidae) revisited: new insights from a molecular phylogeny. *African Journal of Herpetology*, 56, 101–114. https://doi.org/10.1080/21564574.2007.9635557

Han, D., Zhou, K. & Bauer, A.M. (2004) Phylogenetic relationships among gekkotan lizards inferred from c-mos nuclear DNA sequences and a new classification of the Gekkota. *Biological Journal of the Linnean Society*, 83, 353–368. https://doi.org/10.1111/j.1095-8312.2004.00393.x

Ikeuchi, I. & Mori, A. (2014) Natural history of a Madagascan gecko *Blaesodactylus ambonihazo* in a dry deciduous forest. *Current Herpetology*, 33, 161–170. https://doi.org/10.5358/hsj.33.161

Ineich, I. & Bourgoin, T. (2016) Sex and food in a cave during daytime, a possible way to escape predators for the nocturnal Madagascar gekkonid *Paroedura tanjaka* Nussbaum & Raxworthy, 2000. *Herpetology Notes*, 9, 187–190.

Ineich, I., Glaw, F. & Vences, M. (2016) A new species of *Blaesodactylus* (Squamata: Gekkonidae) from Tsingy limestone outcrops in Namoroka National Park, north-western Madagascar. *Zootaxa*, 4109 (5), 523–541. https://doi.org/10.11646/zootaxa.4109.5.2

Jackman, T.R., Bauer, A.M., Greenbaum, E., Glaw, F. & Vences, M. (2008) Molecular phylogenetic relationships among species of the Mal-agasy-Comoran gecko genus *Paroedura* (Squamata: Gekkonidae). *Molecular Phylogenetics and Evolution*, 46, 74–81. https://doi.org/10.1016/j.ympev.2007.10.018

Jenkins, R.K.B., Tognelli, M.F., Bowles, P., Cox, N., Brown, J.L., Chan, L., Andreone, F., Andriamazava, A., Andriantsimanarilafy, R.R., Anjeriniaina, M., Bora, P., Brady, L.D., Hantalalaina, E.F., Glaw, F., Griffiths, R.A., Hilton-Taylor, C., Hoffmann, M., Katariya, V., Rabibisoa, N.H., Rafanomezantsoa, J., Rakotomalala, D., Rakotondravony, H., Rakotondrazafy, N.A., Ralambonirainy, J., Ramanamanjato, J.B., Randriamahazo, H., Randrianantoandro, J.C., Randrianasolo, H.H., Randrianirina, J.E., Randrianizahana, H., Raselimanana, A.P., Rasolohery, A., Ratsoavina, F.M., Raxworthy, C.J., Robsomanitrandrasana, E., Rollande, F., Van Dijk, P.P., Yoder, A.D. & Vences, M. (2014) Extinction risks and the conservation of Madagascar's reptiles. *PLoS One*, 9 (8), e100173. https://doi.org/10.1371/journal.pone.0100173

Jono, T., Bauer, A.M., Brennan, I. & Mori, A. (2015) New species of *Blaesodactylus* (Squamata: Gekkonidae) from Tsingy karstic outcrops in Ankarana National Park, northern Madagascar. *Zootaxa*, 3980 (3), 406–416. https://doi.org/10.11646/zootaxa.3980.3.4

Katoh, K. & Standley, D.M. (2013) MAFFT multiple sequence alignment software version 7: improvements in performance and usability. *Molecular Biology and Evolution*, 30, 772–780. https://doi.org/10.1093/molbev/mst010

Kocher, T.D., Thomas, W.K., Meyer, A., Edwards, S.V., Pääbo, S., Villablanca, F.X. & Wilson, A.C. (1989) Dynamics of mitochondrial DNA evolution in animals: Amplification and sequencing with conserved primers. *Proceedings of the National Academy of Sciences of the USA*, 86, 6196–6200. https://doi.org/10.1073/pnas.86.16.6196

Köhler, J., Vences, M., Scherz, M.D. & Glaw, F. (2019) A new species of nocturnal gecko, genus *Paroedura*, from the karstic Tsingy de Bemaraha formation in western Madagascar. *Salamandra*, 55 (2), 73–81.

Kremen, C., Cameron, A., Moilanen, A., Phillips, S., Thomas, C.D., Beentje, H., Dransfield, J., Fisher, B.L., Glaw, F., Good, T.C., Harper, G.J., Hijmans, R.J., Lees, D.C., Louis Jr. E., Nussbaum, R.A., Raxworthy, C.J., Razafimpahanana, A., Schatz, G.E., Vences, M., Vieites, D.R., Wright, P.C. & Zjhra, M.L. (2008) Aligning conservation priorities across taxa in Madagascar, with high-resolution planning tools. *Science*, 320, 222–226. https://doi.org/10.1126/science.1155193

Kumar, S., Stecher, G. & Tamura, K. (2016) MEGA7: Molecular Evolutionary Genetics Analysis version 7.0 for bigger datasets. *Molecular Biology and Evolution*, 33, 1870–1874. https://doi.org/10.1093/molbev/msw054

Lemme, I., Erbacher, M., Kaffenberger, N., Vences, M. & Köhler, J. (2013) Molecules and morphology suggest cryptic species diversity and an overall complex taxonomy of fish scale geckos, genus *Geckolepis*. *Organisms Diversity and Evolution*, 13, 87–95. https://doi.org/10.1007/s13127-012-0098-y

Moat, J. & Smith, P. (2007) *Atlas of the Vegetation of Madagascar*. Royal Botanic Gardens, Kew Richmond, 124 pp.

Miralles, A., Puillandre, N. Vences, M. (2024) Chapter 4. DNA barcoding in species delimitation: from genetic distances to integrative taxonomy. *In*: de Salle, R. (Ed.), *DNA barcodes: methods and protocols*. *Springer protocol series*. Humana, New York, New York, pp. 77–104. https://doi.org/10.1007/978-1-0716-3581-0_4

Mohan, A.V., Gehring, P.S., Scherz, M.D., Glaw, F., Ratsoavina, F.M. & Vences, M. (2019) Comparative phylogeography and patterns of deep genetic differentiation of two gecko species, *Paroedura gracilis* and *Phelsuma guttata*, across north-eastern Madagascar. *Salamandra*, 55**,** 211–220.

Nachman, M.W., Beckman, E.J., Bowie, R.C., Cicero, C., Conroy, C.J., Dudley, R., Hayes, T.B., Koo, M.S., Lacey, E.A., Martin, C.H., McGuire, J.A., Patton, J.L., Spencer, C.L., Tarvin, R.D., Wake, M.H., Wang, I.J., Achmadi, A., Álvarez-Castañeda, S.T., Andersen, M.J., Arroyave, J., Austin, C.C., Barker, F.K., Barrow, L.N., Barrowclough, G.F., Bates, J., Bauer, A.M.,

Bell, K.C., Bell, R.C., Bronson, A.W., Brown, R.M., Burbrink, F.T., Burns, K.J., Cadena, C.D., Cannatella, D.C., Castoe, T.A., Chakrabarty, P., Colella, J.P., Cook, J.A., Cracraft, J.L., Davis, D.R., Davis Rabosky, A.R., D'Elía, G., Dumbacher, J.P., Dunnum, J.L., Edwards, S.V., Esselstyn, J.A., Faivovich, J., Fjeldså, J., Flores-Villela, O.A., Ford, K, Fuchs, J., Fujita, M.K., Good, J.M., Greenbaum, E., Greene, H.W., Hackett, S., Hamidy, A., Hanken, J., Haryoko, T., Hawkins, M.T., Heaney, L.R., Hillis, D.M., Hollingsworth, B.D., Hornsby, A.D., Hosner, P.A., Irham, M., Jansa, S., Jiménez, R.A., Joseph, L., Kirchman, J.J., LaDuc, T.J., Leaché, A.D., Lessa, E.P., López-Fernández, H., Mason, N.A., McCormack, J.E., McMahan, C.D., Moyle, R.G., Ojeda, R.A., Olson, L.E., Kin Onn, C., Parenti, L.R., Parra-Olea, G., Patterson, B.D., Pauly, G.B., Pavan, S.E., Peterson, A.T., Poe, S., Rabosky, D.L., Raxworthy, C.J., Reddy, S., Rico-Guevara, A., Riyanto, A., Rocha, L.A., Ron, S.R., Rovito, S.M., Rowe, K.C., Rowley, J., Ruane, S., Salazar-Valenzuela, D., Shultz, A.J., Sidlauskas, B., Sikes, D.S., Simmons, N.B., Stiassny, M.L.J., Streicher, J.W., Stuart, B.L., Summers, A.P., Tavera, J., Teta, P., Thompson, C.W., Timm, R.M., Torres-Carvajal, O., Voelker, G., Voss, R.S., Winker, K., Witt, C., Wommack, E.A. & Zink, R.M. (2023) Specimen collection is essential for modern science. *PLoS Biology*, 21, e3002318. https://doi.org/10.1371/journal.pbio.3002318.

Padial, J.M., Miralles, A., De la Riva, I. & Vences, M. (2010) The integrative future of taxonomy. *Frontiers in Zoology*, 7, e16. https://doi.org/10.1186/1742-9994-7-16

Palumbi, S.R., Martin, A., Romano, S., McMillan, W.O., Stice, L. & Grabowski, G. (1991) *The Simple Fool's Guide to PCR. Version 2.0*. Privately published, University of Hawaii, Honolulu, 45 pp.

Penny, S.G., Crottini, A., Andreone, F., Bellati, A., Rakotozafy, L.M.S, Holderied, M.W., Schwitzer, C. & Rosa, G.M. (2017) Combining old and new evidence to increase the known biodiversity value of the Sahamalaza Peninsula, Northwest Madagascar. *Contributions to Zoology*, 86 (4) 273–296. https://doi.org/10.1163/18759866-08604002

Rakotoarimalala, F. & Raselimanana, A.P. (2023) Aperçu global de la tendance de la structure de la communauté herpétofaunique le long du gradient altitudinal du versant Est du Parc National de Marojejy au cours de ces 25 dernières années. *In*: Goodman, S.M. & Raherilalao, M.J. (Eds.), A floral and faunal inventory of the Parc National de Marojejy: Altitudinal gradient and temporal variation. *Malagasy Nature*, 17, pp. 165–186.

Raselimanana, A.P. (2008) Herpétofaune des forêts sèches malgaches. *Malagasy Nature*, 1, 46–75.

Ratsoavina, F.M., Scherz, M.D., Tolley, K.A., Raselimanana, A.P., Glaw, F. & Vences, M. (2019) A new species of *Uroplatus* (Gekkonidae) from Ankarana National Park, Madagascar, of remarkably high genetic divergence. *Zootaxa*, 4683 (1), 84–96. https://doi.org/10.11646/zootaxa.4683.1.4

Rocha, S., Vences, M., Glaw, F., Posada, D. & Harris, D.J. (2009) Multigene phylogeny of Malagasy day geckos of the genus *Phelsuma. Molecular Phylogenetics and Evolution*, 52, 530–537. https://doi.org/10.1016/j.ympev.2009.03.032

Russell, A.P. (1978) The status of the lizard genera *Blaesodactylus* Boettger and *Homopholis* Boulenger (Reptilia: Gekkonidae). *Copeia*, 1978, 25–29. https://doi.org/10.2307/1443817

Scherz, M.D., Daza, J.D., Köhler, J., Vences, M. & Glaw, F. (2017) Off the scale: a new species of fish-scale gecko (Squamata: Gekkonidae: *Geckolepis*) with exceptionally large scales. *PeerJ*, 5, e2955. https://doi.org/10.7717/peerj.2955

Schneider, C.A., Rasband, W.S. & Eliceiri, K.W. (2012) NIH Image to ImageJ: 25 years of image analysis. *Nature Methods*, 9, 671–675. https://doi.org/10.1038/nmeth.2089

Stephens, M., Smith, N.J. & Donnelly, P. (2001) A new statistical method for haplotype reconstruction from population data. *American Journal of Human Genetics*, 68, 978–989. https://doi.org/10.1086/319501

Templeton, A.R., Crandall, K.A. & Sing, C.F. (1992) A cladistic analysis of phenotypic association with haplotypes inferred from restriction endonuclease mapping and DNA sequence data. III. Cladogram estimation. *Genetics*, 132, 619–635. https://doi.org/10.1093/genetics/132.2.619

Uetz, P., Freed, P., Aguilar, R., Reyes, F., Kudera, J. & Hošek, J. (Eds.) (2024) The Reptile Database. Available from: http://www.reptile-database.org (accessed May 15 August 2024)

Vences, M., Miralles, A., Brouillet, S., Ducasse, J., Fedosov, A., Kharchev, V., Kostadinov, I., Kumari, S., Patmanidis, S., Scherz, M.D., Puillandre, N. & Renner, S.S. (2021) iTaxoTools 0.1: Kickstarting a specimen-based software toolkit for taxonomists. *Megataxa*, 6 (2), 77–92. https://doi.org/10.11646/megataxa.6.2.1

Vences, M., Miralles, A. & Dufresnes, C. (2024b) Next-generation species delimitation and taxonomy: implications for biogeography. *Journal of Biogeography*, 51 (9), 1709–1722. https://doi.org/10.1111/jbi.14807

Vences, M., Multzsch, M., Gippner, S., Miralles, A., Crottini, A., Gehring, P.-S., Rakotoarison, A., Ratsoavina, F.M., Glaw, F. & Scherz, M.D. (2022b) Integrative revision of the *Lygodactylus madagascariensis* group reveals an unexpected diversity of little brown geckos in Madagascar's rainforest. *Zootaxa*, 5179 (1), 1–61. https://doi.org/10.11646/zootaxa.5179.1.1

Vences, M., Patmanidis, S., Kharchev, V. & Renner, S.S. (2022a) Concatenator, a user-friendly program to concatenate DNA sequences, implementing graphical user interfaces for MAFFT and FastTree. *Bioinformatics Advances*, 2, vbac050. https://doi.org/10.1093/bioadv/vbac050

Vences, M., Patmanidis, S., Schmidt, J.-C., Matschiner, M., Miralles, A. & Renner, S.S. (2024a) Hapsolutely: a user-friendly tool integrating haplotype phasing, network construction and haploweb calculation. *Bioinformatics Advances*, vbae083. https://doi.org/10.1093/bioadv/vbae083